

Insertion Reactions of Square-Planar Diorganoplatinum.

1. Scope and Mechanisms of Stereoselective Carbonylation, Decarbonylation, and Relevant Reactions of Alkyl Acyl, Aryl Acyl, Alkyl α -Ketoacyl, Aryl α -Ketoacyl, Diacyl, and Acyl α -Ketoacyl Complexes[†]

Jwu-Ting Chen,* Yu-Sung Yeh, Ching-Shuenn Yang, Fu-Yu Tsai, Gwo-Liang Huang, Bor-Chyr Shu, Tsang-Miao Huang, Yan-Su Chen, Gene-Hsiang Lee, Ming-Chu Cheng, Chih-Chieh Wang, and Yu Wang

Department of Chemistry, National Taiwan University, Taipei, Taiwan 106, Republic of China

Received August 16, 1994[®]

Transmetalation between *trans*-Pt(COR)(X)(PPh₃)₂ (R = Me, Et, Ph; X = halide) and R'₂Zn (R' = Me, Et, Ph) in benzene or toluene at 25 °C readily results in the formation of *trans*-Pt(COR)(R')(PPh₃)₂ in high yields. Alkylation of *trans*-Pt(COCOR)(OTf)(PPh₃)₂ or *trans*-[Pt(COCOR)(L)(PPh₃)₂]⁺ (L = H₂O, THF; R = Me, Et, Ph, OMe) with use of R'₂Zn (R = Me, Et, Ph) provides *trans*-Pt(COCOR)(R')(PPh₃)₂. Carbonylation of *trans*-Pt(COR)(R')(PPh₃)₂ exclusively gives *cis*-Pt(COR)(COR')(PPh₃)₂ in quantitative yields with its reactivity following the order R' = Et >> Ph > Me. An alternative synthetic route to the *cis* diacyl complexes, albeit in low yields, is by means of the nucleophilic addition of LiR' or R'MgX to the *cis*-[Pt(COR)(CO)(PPh₃)₂]⁺ cation. With the assistance of CO, *cis*-Pt(COEt)(COMe)(PPh₃)₂ undergoes reversible intermolecular acyl scrambling to form *cis*-Pt(COMe)₂(PPh₃)₂ and *cis*-Pt(COEt)₂(PPh₃)₂, reaching the equilibrium ratio 2:1:1. CO also promotes isomerization of *trans*-Pt(Me)(CO₂Me)(PPh₃)₂ to its *cis* derivative, which suffers substitution of CO for PPh₃ to produce (*SP*-4-2)- and (*SP*-4-4)-Pt(PPh₃)(CO₂Me)(CO)(Me). The stereoselective carbonylation of *trans*-Pt(COCOR)(R')(PPh₃)₂ exclusively affords novel *cis*-Pt(COCOR)(COR')(PPh₃)₂ in quantitative yields. The reactivity also follows the order R' = Et >> Ph > Me. The mechanism of carbonylation of the *trans* diorganoplatinum complexes is likely led by a reversible substitution of CO for a PPh₃ ligand, followed by alkyl (or aryl) migration from metal to CO and subsequent recoordination of PPh₃. At 25 °C, *trans*-Pt(COCOR)(R')(PPh₃)₂ can spontaneously transform to *trans*-Pt(COR')(COR)(PPh₃)₂. In a comparable sense, *trans*-Pt(COR)(R')(PPh₃)₂ species (R = Me, R' = Et; R = Ph, R' = Me, Et) convert to *trans*-Pt(COR')(R)(PPh₃)₂ irreversibly at 50 °C. Such reactions likely proceed via a five-coordinate intermediate by intramolecular CO transfer. The methoxyoxalyl derivatives *trans*-Pt(COCO₂Me)(R')(PPh₃)₂ are also subject to decarbonylation, resulting in *cis*-Pt(CO₂Me)(R')(PPh₃)₂ instead. Thermolysis of the *cis* diacyl complexes leads to the formation of C(O)-C(O) bonds, yielding vicinal diketones. The *cis* acyl α -ketoacyl complexes first suffer decarbonylation to form the *trans* diacyl complexes, which succeedingly convert to *trans* acyl carboxylato complexes, *trans*-Pt(COR')(OCOR)(PPh₃)₂ and *trans*-Pt(OCOR')(COR)(PPh₃)₂, in solutions with moisture, as well as organic ketones or diketones. The X-ray crystallographic analyses for all title species and a carboxylato complex are provided.

Introduction

The reactions of carbonylation and decarbonylation of the d⁸ square-planar complexes of group 10 metals are of considerable importance to organic functionalization and catalysis.¹ Relevant mechanistic studies of

such reactions have been largely focused on monoorgano complexes. For instance, it has been shown that the typical species M(R)(X)L₂ (M = Ni, Pd, Pt; R = alkyl, aryl; X = halide; L = monodentate phosphine, arsine, etc.) react with CO to yield acyl species M(COR)(X)L₂ with only the thermodynamically stable *trans* configuration.² There has been no example of *cis* acyl derivative that results from carbonylation, unless bidentate ligand is involved.³

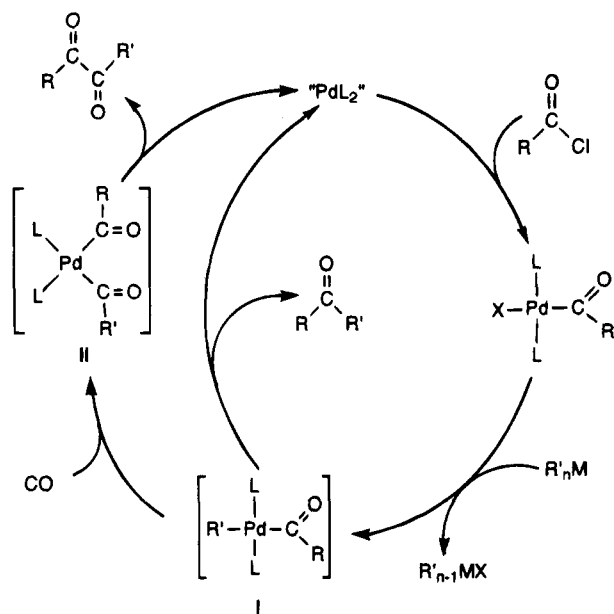
[†] Partially based on the Ph.D. thesis of Y.-S.Y., National Taiwan University, 1992.

[®] Abstract published in *Advance ACS Abstracts*, October 15, 1994.

(1) (a) Colquhoun, H. M.; Thompson, D. J.; Twigg, M. V. *Carbonylation: Direct Synthesis of Carbonyl Compounds*; Plenum Press: New York, 1991. (b) *Comprehensive Organometallic Chemistry*; Wilkinson, G., Ed.; Pergamon Press: Oxford, England, 1982; Vol. 6 and 8. (c) Heck, R. F. *Organotransition Metal Chemistry*; Academic Press: New York, 1974. (d) Tsuji, T. *Organic Synthesis by Means of Transition Metal Complexes*; Springer-Verlag: Berlin, Heiderberg, New York, 1975. (e) Collman, J. P.; Hegedus, L. S.; Norton, J. R.; Finke, R. G. *Principles & Applications of Organotransition Metal Chemistry*; University Science Books: Mill Valley, CA, 1987.

(2) (a) Booth, G.; Chatt, J. *J. Chem. Soc. A* **1966**, 634. (b) Clark, H. C.; Puddephatt, R. *J. Inorg. Chem.* **1970**, *9*, 2670. (c) Glyde, R. W.; Mawby, R. *J. Inorg. Chem.* **1971**, *10*, 854. (d) Wilson, C. J.; Green, M.; Mawby, R. *J. Chem. Soc. A* **1974**, *421*, 1293. (e) Garrou, P. E.; Heck, R. F. *J. Am. Chem. Soc.* **1976**, *98*, 4115. (f) Sugita, N.; Minkiewicz, J. V.; Heck, R. F. *Inorg. Chem.* **1978**, *17*, 2809. (g) Anderson, G. K.; Cross, R. *J. Chem. Soc. A* **1980**, *712*, 1434. (h) Anderson, G. K.; Cross, R. *J. Acc. Chem. Res.* **1984**, *17*, 67 and references therein.

Scheme 1



Carbonylation and decarbonylation in square-planar diorganoplatinum systems, particularly those containing acyl ligands, has been nearly unexplored.⁴ Well-characterized acyl alkyl and diacyl complexes of such systems were actually unprecedented prior to our communication,⁵ although involvement of these species in the group 10 metal-mediated reactions of carbonylation and double carbonylation has been considered. The Pd-catalyzed coupling reactions of acid chloride with organotin reagents have been proved to be very useful for the synthesis of ketones.⁶ The mechanistic studies suggested that acyl(alkyl)palladium complexes (I in Scheme 1), presumably resulting from transmetalation between the acylhalopalladium and organotin compounds, might be a crucial intermediate in these reactions. However, no detection of I or its platinum analog has been made. Tanaka also reported the reactions of carbonylative coupling between organozinc and acid halide, yielding diketones and related products, and proposed a mechanism involving an intermediate diacyl species (II in Scheme 1), still without direct evidence.⁷

The paucity of trans diorganoplatinum complexes, particularly those containing acyl ligands, has been partially ascribed to the fact that the complexes having ligands with

high trans influence at the trans coordination sites are congenitally unfavored.^{8,9} Besides, the synthetic strategy for such species is still confined to conventional transmetalation with main-group organometallic among species, which the acyl reagents are not readily available.¹⁰ Our previous results on the formation of *trans*-Pt(COPh)(COEt)(PPh₃)₂ from *trans*-Pt(COCOPh)(Et)(PPh₃)₂ have demonstrated that trans diorganoplatinum complexes can be reasonably stable under suitable conditions¹¹ and has prompted us to extend this synthetic work to other trans alkyl α -ketoacyl and alkyl acyl derivatives. It has been found that these four-coordinate trans diorganoplatinum complexes can undergo efficient stereoselective carbonylation under rather mild conditions, leading to novel cis diacyl and cis acyl α -ketoacyl complexes, respectively, and eventually to diketones and ketones.¹² Such results not only reveal the intriguing reactivity of new diorganoplatinum complexes of platinum(II) but also provide a good model for the Pd-catalyzed coupling and carbonylative coupling reactions of acid halides with organometals. From a mechanistic viewpoint, the stereoselective carbonylation and decarbonylation in such diorganoplatinum complexes are also worthy of a closer look. In this article, we report the synthesis, structures, and reactivity of the new acyl alkyl, alkyl α -ketoacyl, diacyl, acyl α -ketoacyl, and related complexes of platinum(II). The reaction scope and mechanisms of carbonylation, decarbonylation, and the relevant reactions are discussed.

Results

Synthesis and Characterization of *trans*-Pt(COR)(R')(PPh₃)₂. Synthesis of the trans acyl alkyl and acyl aryl complexes has been conducted by convenient transmetalation between *trans*-Pt(COR)(X)(PPh₃)₂ and diorganozinc reagents. The starting acyl halo complexes were prepared according to documented methods.¹³ In typical experiments, treatment of *trans*-Pt(COR)(Cl)(PPh₃)₂ (R = Me (**1a**), Et (**1b**), Ph (**1c**)) with R'₂Zn in benzene or toluene under a nitrogen atmosphere at 25 °C readily resulted in the formation of yellow *trans*-Pt(COR)(R')(PPh₃)₂ (R' = Me, R = Me (**2a**), Et (**2b**), Ph (**2c**); R' = Et, R = Me (**3a**), Et (**3b**), Ph (**3c**); R' = Ph, R = Me (**4a**), Et (**4b**), Ph (**4c**)), as illustrated in Scheme 2. Most of the acyl alkyl complexes were precipitated by *n*-hexane from the reaction solutions to give excellent yields. The methyl derivatives were generally formed along with substantial amounts of *cis*-Pt(Me)₂(PPh₃)₂. The desired products **2a–c** were purified satisfactorily by silica gel column chromatography with Et₂O/benzene solutions as the eluent. In chloroform, *trans*-Pt(COR)(R')(PPh₃)₂ slowly transforms to *trans*-Pt(COR)(Cl)(PPh₃)₂, presumably due to the reaction with HCl in the solvent.

(8) Appleton, T. G.; Clark, H. C.; Manzer, L. E. *Coord. Chem. Rev.* **1973**, *10*, 335.

(9) (a) Yamamoto, A. *Organotransition Metal Chemistry: Fundamental Concepts and Applications*; Wiley: New York, 1986; Chapter 6. (b) Anderson, G. K.; Clark, H. C.; Davies, J. A. *Inorg. Chem.* **1981**, *20*, 3607.

(10) (a) Wakefield, B. J. *Organolithium Methods*; Academic Press: London, San Diego, CA, 1988. (b) Seyferth, D.; Weinstein, R. M.; Wang, W.-L.; Hui, R. C.; Archer, C. M. *Isr. J. Chem.* **1984**, *24*, 167.

(11) Chen, J.-T.; Huang, T.-M.; Cheng, M.-C.; Wang, Y. *Organometallics* **1991**, *10*, 2838.

(12) Huang, G.-L.; Huang, T.-M.; Chen, J.-T.; Lee, G.-H.; Wang, Y. *Inorg. Chem.* **1992**, *30*, 4034.

(13) Kubota, M.; Rothrock, R. K.; Geibel, J. J. *Chem. Soc. A* **1973**, 1267.

(3) (a) Bryndza, H. E.; Tam, W. *Chem. Rev.* **1988**, *88*, 1163. (b) Bryndza, H. E.; Kretchmar, S. A.; Tulip, T. H. *J. Chem. Soc., Chem. Commun.* **1985**, 977. (c) Bryndza, H. E. *Organometallics* **1985**, *4*, 406. (d) Bennett, M. A.; Rokicki, A. *Organometallics* **1985**, *4*, 180. (e) Bennett, M. A.; Robertson, G. B.; Whimp, P. O.; Yoshida, T. *J. Am. Chem. Soc.* **1973**, *95*, 3028. (f) van Leeuwen, P. W. N. M.; Roobeek, C. F.; Wife, R. L.; Frijns, J. H. G. *J. Chem. Soc., Chem. Commun.* **1986**, 31. (g) van Leeuwen, P. W. N. M.; Roobeek, C. F.; Frijns, J. H. G.; Orpen, A. G. *Organometallics* **1990**, *9*, 1211. (h) Dekker, G. P. C.; Buijs, A.; Elsevier, C. J.; Vrieze, K.; van Leeuwen, P. W. N. M.; Smeets, W. J. J.; Spek, A. L.; Wang, Y. F.; Stam, C. H. *Organometallics* **1992**, *11*, 1937. (i) Davcid, Y. B.; Portnoy, M.; Milstein, D. *J. Am. Chem. Soc.* **1989**, *111*, 8742. (j) Dekker, D. P. C. M.; Buijs, A.; Elsevier, C. J.; Vrieze, K.; van Leeuwen, P. W. N. M.; Smeets, W. J. J.; Spek, A. L.; Wang, Y. F.; Stam, C. H. *Organometallics* **1992**, *11*, 1937. (k) Portnoy, M.; Milstein, D. *Organometallics* **1993**, *12*, 1655.

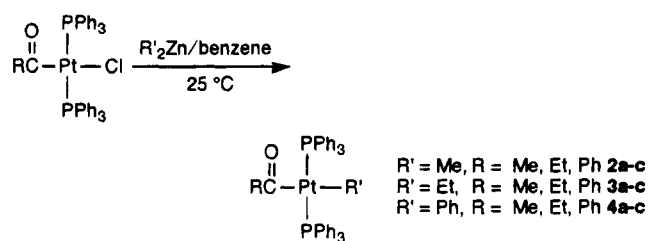
(4) (a) Ozawa, F.; Yamamoto, A. *Chem. Lett.* **1981**, 289. (b) Ozawa, F.; Ito, T.; Yamamoto, A. *J. Am. Chem. Soc.* **1980**, *102*, 6457.

(5) A preliminary communication has been published: Chen, J.-T.; Huang, T.-M.; Cheng, M.-C.; Wang, Y. *Organometallics* **1990**, *9*, 539.

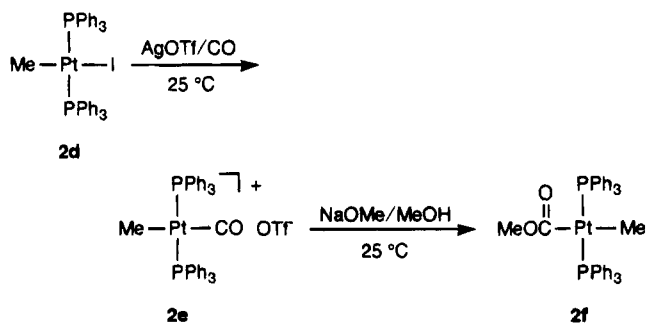
(6) (a) Tanaka, M. *Tetrahedron Lett.* **1979**, 2601. (b) Labadie, J. W.; Stille, J. K. *J. Am. Chem. Soc.* **1983**, *105*, 6129.

(7) Yamashita, H.; Kobayashi, T.; Sakakura, T.; Tanaka, M. *J. Organomet. Chem.* **1988**, *356*, 125.

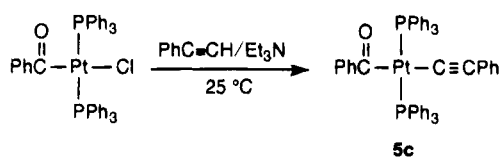
Scheme 2



Scheme 3



Scheme 4



The acyl carbonyls in *trans*-Pt(COR)(R')(PPh₃)₂ often exhibit stretching absorptions lower than 1600 cm⁻¹ in their infrared spectra. The relatively low stretching frequency of the C=O bond in comparison with that of the acyl C=O in *trans*-Pt(COR)(X)(PPh₃)₂ is ascribed to the fact that the R' groups of σ -donor, unlike halides, lack of competition with the Pt–acyl bond for π -interaction. The ¹³C NMR spectra show that the α -carbon of the acyl ligand of *trans*-Pt(COPh)(Me)(PPh₃)₂ is further downfield than that of *trans*-Pt(COPh)(Cl)(PPh₃)₂ (δ 262.2 versus 212.5). Such data indicate that the back- π -donation from metal to the acyl group in *trans*-Pt(COR)(R')(PPh₃)₂ may be significant. The $J_{\text{H-Pt}}$ values corresponding to the α -hydrogen of R' are in the region of 40–50 Hz.

The methoxycarbonyl methyl derivative *trans*-Pt(CO₂Me)(Me)(PPh₃)₂ (**2f**) was acquired via nucleophilic addition of methoxide ion to *trans*-[Pt(Me)(CO)(PPh₃)₂](OTf) (**2e**), as shown in Scheme 3. Complex **2e** was prepared by abstraction of iodide ion from *trans*-Pt(Me)(I)(PPh₃)₂ (**2d**) with use of silver trifluoromethanesulfonate (AgOTf) in the presence of CO. The acetylide derivative *trans*-Pt(COPh)(C \equiv CPh)(PPh₃)₂ (**5c**) was prepared by the reaction of **1c** and phenylacetylene with the assistance of Et₃N (Scheme 4).

The single-crystal structures of complexes **3c**, **4b,c**, and **5c** were determined by X-ray diffraction. The ORTEP drawings of the two "isomers" **3c** and **4b** (vide supra) are shown in Figure 1. Their crystallographic data and important bond parameters are collected in the Experimental Section. The rest of the data are supplied in the supplementary material. The distances of M–C(alkyl) and M–C(aryl) bonds are slightly longer than the M–C(acyl) bonds. The acyl plane (Pt–C–O) is roughly perpendicular to the molecular plane, with

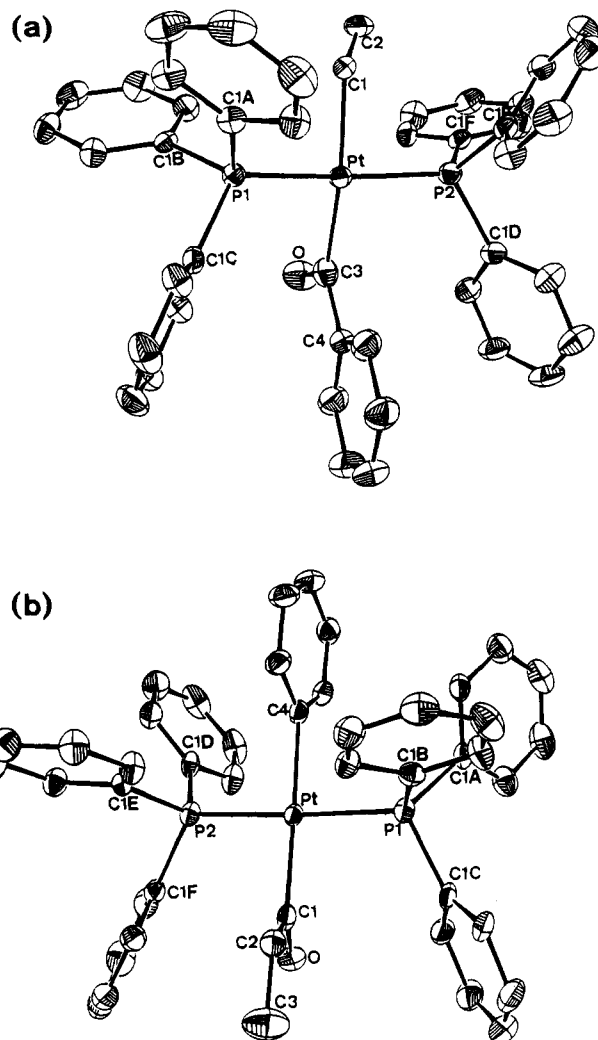


Figure 1. ORTEP drawings of transpositional isomers (a) *trans*-Pt(COPh)(Et)(PPh₃)₂ (**3c**) and (b) *trans*-Pt(COEt)(Ph)(PPh₃)₂ (**4b**). (All H atoms are omitted for clarity.)

the dihedral angle being 88.3(6)° for **3c**, 76.1(7)° for **4b**, 99.3(7)° for **4c**, and 94.5(5)° for **5c**. The acetylide ligand of **5c** is linear with $\angle\text{Pt-C8-C9} = 174.9(6)^\circ$ and $\angle\text{C8-C9-C10} = 176.8(7)^\circ$. The length of the Pt–C(acetylide) bond (2.077(5) Å) falls in the long range for platinum acetylides (1.9–2.1 Å), suggesting that the *trans* influence of the benzoyl ligand is rather strong.⁸ The distance of the C \equiv C bond (1.098(8) Å) thus is relatively short among platinum acetylides (1.07–1.22 Å).¹⁴

Transpositional Isomerization of *trans*-Pt(COR)(R')(PPh₃)₂. At 50 °C in benzene, *trans*-Pt(Et)(COMe)(PPh₃)₂ (**3a**) was found to transform to *trans*-Pt(COEt)(Me)(PPh₃)₂ (**2b**). The conversion was over 80% within 2 h, and the rest of **3a** decomposed to MeC(O)Et (Scheme 5). Complex **2b** did not revert to **3a** under similar conditions. Complexes **2b** and **3a** are the isomers with the methyl and ethyl groups transposed between the adjacent carbonyl carbon and Pt atom. An analogous transformation from **2c** to **4a** along with formation of acetophenone was also observed at 54 °C. However, the inorganic and organic species only reached the ratio 5:1:1 after 5 h. After a 9-h heating, over 90% of **2c** decomposed to PhC(O)Me, with only a trace of **4a**

(14) Furlani, A.; Licocchia, S.; Russo, M. V. *J. Chem. Soc., Dalton Trans.* **1982**, 2449.

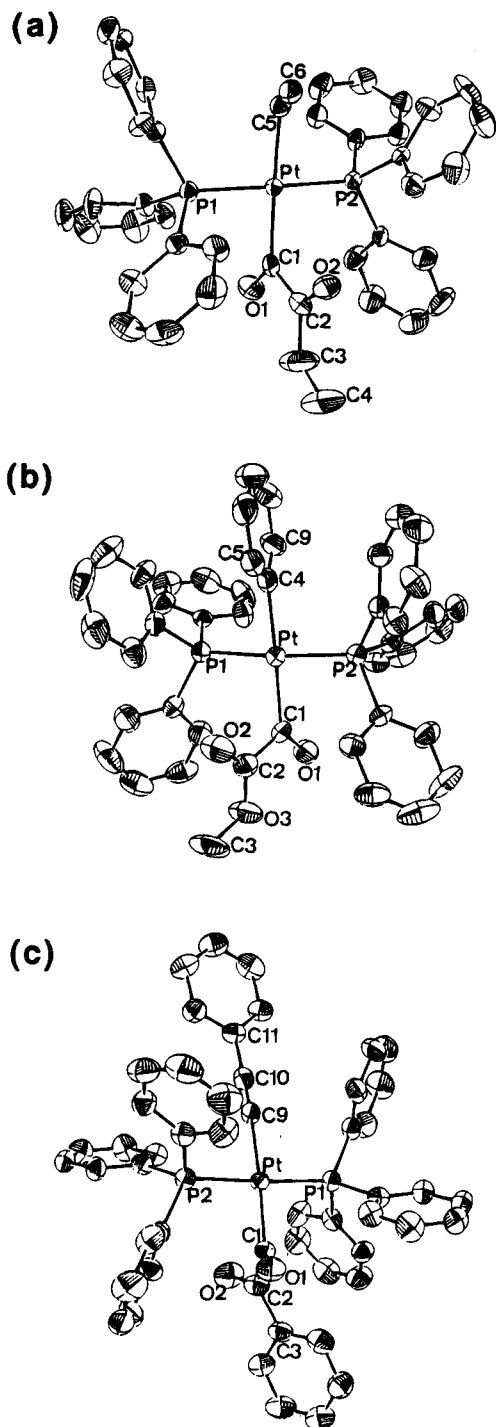
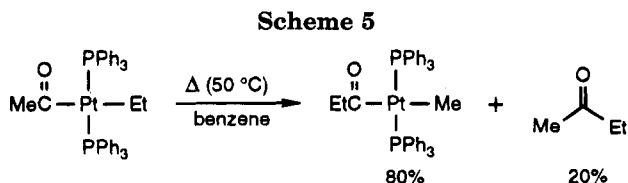
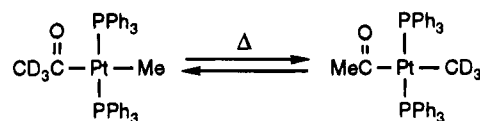


Figure 2. ORTEP drawings of *trans*-Pt(COCOR)(R')(PPh₃)₂: (a) **14b**; (b) **15d**; (c) **16c**. (All H atoms are omitted for clarity.)



being detected. The reverse reaction of **4a** to **2c** never had a chance to build up to a detectable extent before **4a** decomposed to PhC(O)Me. When complex **3c** was heated to 50 °C, **4b** and PhC(O)Et appeared at a rate similar to that for the analogous reaction of **2c**. The amount of **4b** was never over 30% of the starting

Scheme 6

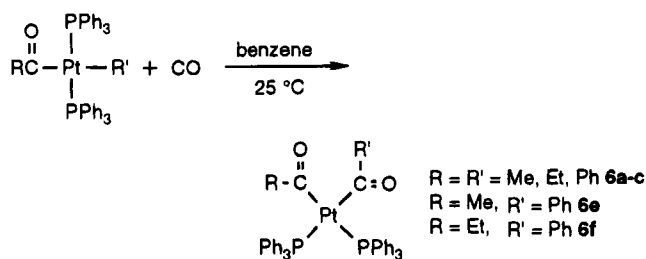
amounts of **3c** through the course of the reaction. PhC(O)Et was the only end product. While the reaction was carried out in the presence of acrylonitrile, the rate of ketone formation from **4b** markedly increased.¹⁵ However, the transformation of **3c** to **4b** was not influenced by the addition of CH₂CHCN. The isomerization of *trans*-Pt(COCD₃)(Me)(PPh₃)₂ (*d*₃-acetyl-**2a**) to *trans*-Pt(COMe)(CD₃)(PPh₃)₂ (*d*₃-Me-**2a**) at 44 °C reached a 1:1 ratio within 1 h. The relative amounts of these two complexes remained unchanged after 4 h. However, *trans*- and *cis*-Pt(Me)(*d*₃-Me)(PPh₃)₂ continued to increase at the expense of total *d*₃-**2a**. These results indicate the reversibility of transposition between *d*₃-acetyl-**2a** and *d*₃-Me-**2a** (Scheme 6). Similar ethyl (and *d*₅-ethyl) scrambling in *trans*-Pt(COC₂D₅)(Et)(PPh₃)₂ was never observed.

Formation of *cis*-Pt(COR)(COR')(PPh₃)₂ via Stereoselective Carbonylation of *trans*-Pt(R')(COR)(PPh₃)₂. When a *d*₆-benzene solution containing *trans*-Pt(COPh)(Et)(PPh₃)₂ (**3c**) was exposed to CO, the immediate measurement of the ³¹P NMR exhibited complete conversion from a singlet to a pair of doublets at δ 14.9 and 15.3 with *J*_{Pt-P} = 1695 and 1561 Hz, respectively. Longer exposure to CO (for instance, bubbling CO through the solution for 15 min or even longer) did not cause any further change. The reaction of *trans*-Pt(COEt)(Ph)(PPh₃)₂ (**4b**) with CO gave the same results but took nearly 1 h to complete. Both reactions were exclusive. The doublets of doublets of ³¹P resonances indicate that the product (designated as **6f**) contains two phosphines occupying the *cis* sites in a square-planar geometry. The values of *J*_{Pt-P} suggest that both phosphines are *trans* to the acyl ligands.⁵ The IR spectrum of **6f**, which comprises two carbonyl absorption lines at 1604 and 1622 cm⁻¹, and its ¹H NMR spectrum also support the existence of two acyl ligands. The reaction of **3c** and ¹³CO showed that external ¹³CO was incorporated only in the resulting propionyl ligand. Such carbonylation reactions could be substantially retarded when PPh₃ was present; increasing CO enhances the reaction rate.

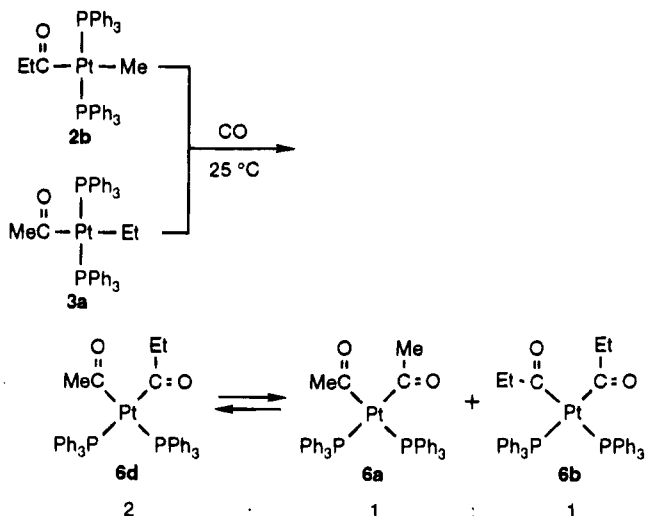
The reaction of *trans*-Pt(COEt)(Et)(PPh₃)₂ (**3b**) with CO led to a single product, for which the ³¹P resonance was a singlet at δ 14.9 with *J*_{Pt-P} = 1568 Hz, indicating that the two PPh₃ ligands are magnetically equivalent. The ³¹P NMR data of the products obtained from the reactions of *trans*-Pt(COMe)(Me)(PPh₃)₂ (**4a**) or *trans*-Pt(COPh)(Ph)(PPh₃)₂ with CO were observed at δ 14.0 (*J*_{Pt-P} = 1558 Hz) and δ 14.1 (*J*_{Pt-P} = 1600 Hz). They are thus identified as *cis*-Pt(COR)₂(PPh₃)₂ (R = Me (**6a**), Et (**6b**), Ph (**6c**)) (Scheme 7). The carbonylation rate for the phenyl derivative is slightly faster than that for the methyl complex but markedly slower than for all ethyl derivatives under the same conditions. No carbonylation of the acetylide complex **5c** was observed.

(15) (a) Tatsumi, K.; Hoffmann, R.; Yamamoto, A.; Stille, J. K. *Bull. Chem. Soc. Jpn.* **1981**, *54*, 1857. (b) Yamamoto, A. *Organotransition Metal Chemistry: Fundamental Concepts and Applications*; Wiley: New York, 1986; Chapter 6.

Scheme 7



Scheme 8



When a solution of *trans*-Pt(COMe)(Et)(PPh₃)₂ (**3a**) was briefly exposed to trace CO, transformation of **3a** to *cis*-Pt(COMe)(COEt)(PPh₃)₂ (**6d**) was accomplished. Bubbling CO through a solution of **3a** for 10 min afforded not only **6d**, as expected, but surprisingly also **6a,b** in the ratio 2:1:1. Similar treatment of *trans*-Pt(COEt)(Me)(PPh₃)₂ (**2b**) in the presence of sufficient CO led to the same results of acyl scrambling. Direct reaction of **6d** with CO or mixing of equal amounts of **6a** and **6b** with CO for 10 min also resulted in the three diacyl complexes with the same relative abundance. These reactions are summarized in Scheme 8. No reaction ever occurs, if CO is not provided. The carbonylation of *trans*-Pt(COPh)(Me)(PPh₃)₂ (**2c**) similarly yielded **6e**, **6a**, and **6c**, however, in the ratio 5.5:1.5:1 in over 90% total conversion. The addition of PPh₃ to the reaction solutions severely retarded such carbonylative acyl scrambling. A detailed study of such reactions will be reported in a separate paper.

X-ray diffraction confirmed the structure of **6f**, and its ORTEP diagram is shown in Figure 3a. The four ligands and the metal are in a distorted-square-planar configuration, and the two acyl ligands are in a cis disposition, with $\angle\text{C1-Pt-C4}$ being only 81.6(9)°. Such a small angle causes the distance between the C1 and C4 atoms to be only 2.67(3) Å. Both acyl planes (Pt-C1-O1 and Pt-C4-O2) are nearly perpendicular to the molecular plane (P1-P2-C4-C1), with the dihedral angles being 97(2) and 93(2)°, respectively. The two acyl carbonyls are *s-trans* to each other with a torsional angle (O1-C1-C4-O2) of 138(3)°. Other bonding parameters are similar to those of the dibenzoyl analog.⁵

Instead of undergoing carbonylation, *trans*-Pt(CO₂Me)(Me)(PPh₃)₂ (**2f**) isomerizes to its *cis* derivative **2f'** in over 80% yield within a few hours in the presence of

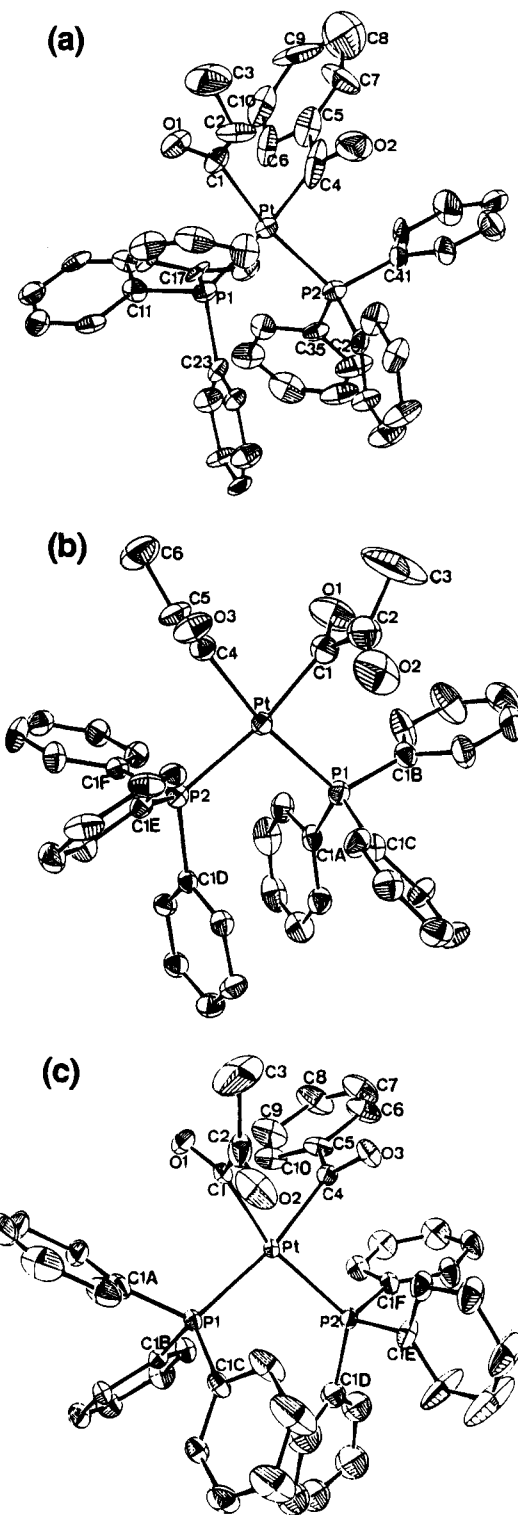
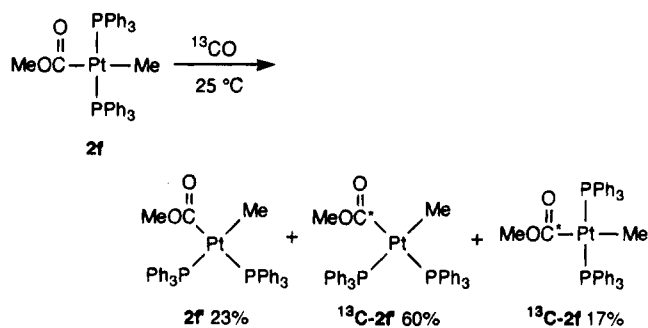


Figure 3. ORTEP drawings of (a) *cis*-Pt(COPh)(COEt)-(PPh₃)₂ (**6f**), (b) *cis*-Pt(COEt)(COCOMe)(PPh₃)₂ (**17a**), and (c) *cis*-Pt(COPh)(COCOMe)(PPh₃)₂ (**18a**). (All H atoms are omitted for clarity.)

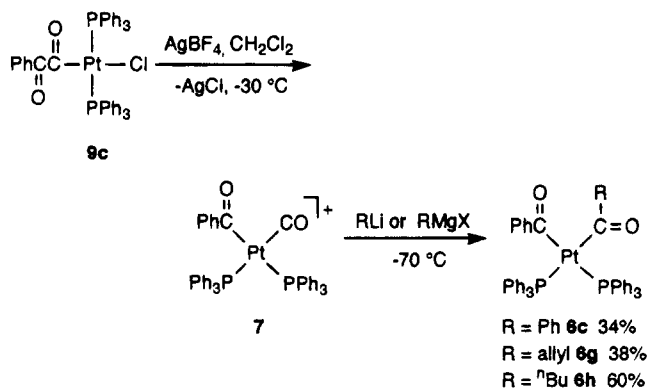
CO. No reaction was observed after 1 day, when external CO was not provided. When ¹³CO was used, the complexes **2f'** and the labeled *cis* (¹³C-**2f'**) and *trans* (¹³C-**2f**) derivatives in the ratio 23:60:17 were acquired (based on the data of NMR integrations) (Scheme 9). Further bubbling of CO into the solution causes the occurrence of (*SP*-4-2)- and (*SP*-4-4)-Pt(PPh₃)(CO₂Me)-(CO)(Me) (**8b** and **8b'**) (vide supra, Scheme 15).

Formation of *cis*-Pt(COR)(COR')(PPh₃)₂ by Nu-

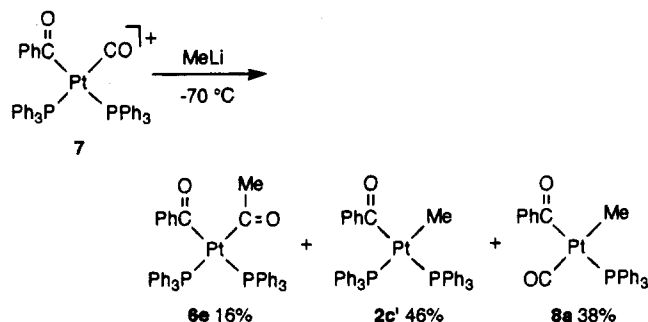
Scheme 9



Scheme 10

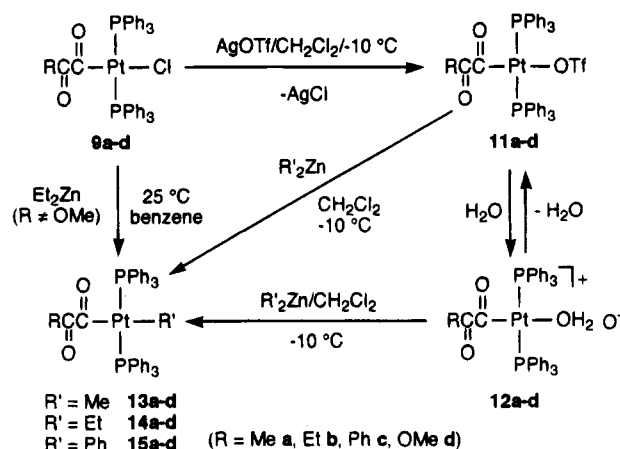


Scheme 11



Electrophilic Addition of Carbanion to *cis*-[Pt(COR)(CO)(PPh₃)₂]⁺. Abstraction of chloride from *trans*-Pt(COCOPh)(Cl)(PPh₃)₂ with AgBF₄ in dichloromethane at -29 °C led to formation of *cis*-[Pt(COPh)(CO)(PPh₃)₂]⁺(BF₄⁻) (**7**).¹⁶ The reactions of complex **7** with PhLi or RMgCl (R = allyl, ⁿBu) provide a complementary route to *cis*-Pt(COPh)(COR)(PPh₃)₂ (R = Ph (**6c**), allyl (**6g**), ⁿBu (**6h**), respectively), albeit in low yields (generally <40%) (Scheme 10). The single-crystal X-ray structure of **6c** was determined and reported in a prior communication.⁵ In the reaction of **7** and MeLi, *cis*-Pt(COPh)(Me)(PPh₃)₂ (**2c'**) and (*SP*-4-3)-Pt(PPh₃)(CO)(COPh)(CH₃) (**8a**) were formed along with **6e** in a ratio 2.5:3:1 in 55% conversion (Scheme 11). When this reaction was carried out in the presence of an extra 2 equiv of PPh₃, only **2c'** and **8a** were obtained in 1:3.5 relative yields, and the total conversion was raised to 90%. Both **8a** and **2c'** have been isolated and characterized spectroscopically and crystallographically.⁵ Addition of PPh₃ to a solution of **8a** readily results in complete conversion to **2c'**. Bubbling CO into a solution

Scheme 12



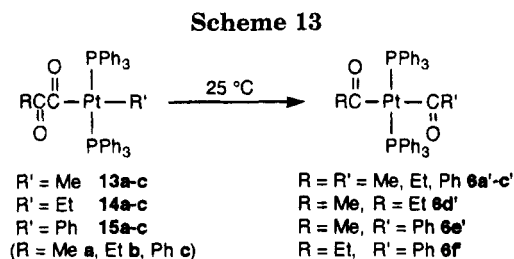
of **2c'** slowly caused the appearance of **8a** and its isomer (*SP*-4-4)-Pt(PPh₃)(CO)(COPh)(CH₃) (**8a'**). The interconversion between **6e** and **2c'** has never been detected. Instead, both complexes thermally decomposed to acetophenone.

Synthesis and Characterization of *trans*-Pt(COCOR)(R')(PPh₃)₂. It has been previously found that ethylation of [*trans*-Pt(COCOPh)(THF)(PPh₃)₂](BF₄) (**10c**) with Et₂Zn results in *trans*-Pt(Et)(COCOPh)(PPh₃)₂ (**14c**).¹¹ Due to the unfortunate solubility of the THF derivatives in common organic solvents, a modified procedure in which *trans*-Pt(COCOR)(OTf)(PPh₃)₂ (OTf = OSO₂CF₃; R = Me (**11a**), Et (**11b**), Ph (**11c**), OMe (**11d**)) or [*trans*-Pt(COCOR)(H₂O)(PPh₃)₂](OTf) (**12a-d**)¹⁷ were used instead has been established for the synthesis of other derivatives of **14c**. Ethylation of complexes **11a-d** or **12a-d** with use of Et₂Zn led to *trans*-Pt(COCOR)(Et)(PPh₃)₂ (**14a-d**) in high yield (>70%). Transmetalation between *trans*-Pt(COCOR)(Cl)(PPh₃)₂ (**9a-c**) and Et₂Zn also feasibly affords the α-ketoacyl ethyl complexes **14a-c** in good yields (~70%). However, the reaction of *trans*-Pt(COCO₂Me)(Cl)(PPh₃)₂ (**9d**) with Et₂Zn was complicated. *trans*-Pt(COCOR)(Me)(PPh₃)₂ (**13a-d**) and *trans*-Pt(COCOR)(Ph)(PPh₃)₂ (**15a-d**) were prepared from the reactions of **11a-d** or **12a-d** with Ph₂Zn or Me₂Zn, respectively. Relatively low yields were obtained in such cases (Scheme 12). In the reactions of **9a-c** with Me₂Zn or Ph₂Zn, the desired products **13a-c** and **15a-c** resulted along with the dimethyl or diphenyl products *cis*-PtR₂(PPh₃)₂, which severely interfered with the purification and lowered the yields of the target compounds. The acetylide complex *trans*-Pt(COCOPh)(C≡CPh)(PPh₃)₂ (**16c**) was prepared according to a procedure similar to that used for preparing the benzoyl analog **5c**.

A feature of *trans*-Pt(COCOR)(R')(PPh₃)₂ (except R = OMe) that distinguishes these species from most of the known organoplatinum complexes is their striking purple appearance. Complexes **13-15(a-c)** generally exhibit a long-wavelength MLCT band in the region over 530 nm, which is about 200 nm longer than the corresponding absorption of the acyl analogs **2-4(a-c)**. The infrared spectra of such complexes, as for other α-ketoacyl complexes, comprise two well-resolved car-

(16) (a) Huang, T.-M.; Chen, J.-T.; Lee, G.-H.; Wang, Y. *Organometallics* **1991**, *10*, 175. (b) Sen, A.; Chen, J.-T.; Vetter, W. M.; Whittle, R. R. *J. Am. Chem. Soc.* **1997**, *119*, 148.

(17) (a) Chen, J.-T.; Yeh, Y.-S.; Tzeng, W.-H.; Huang, T.-M.; Cheng, M.-C.; Lee, G.-H.; Wang, Y. *J. Chin. Chem. Soc.* **1991**, *38*, 573. (b) Chen, J.-T.; Yeh, Y.-S.; Lee, G.-H.; Wang, Y. *J. Organomet. Chem.* **1991**, *414*, C64.



bonyl stretching bands. The frequency with respect to α -CO is lower than 1600 cm^{-1} , which is similar to those of $\text{trans-Pt}(\text{COR})(\text{R}')(\text{PPh}_3)_2$. The ^{13}C NMR spectrum of **13d** consists of the resonances of α -CO at δ 237.1 ($J_{\text{C-Pt}} = 844 \text{ Hz}$), of β -CO at δ 168.7 ($J_{\text{C-Pt}} = 129 \text{ Hz}$), and of the methyl ligand at δ -8.6 ($J_{\text{C-P}} = 9.1 \text{ Hz}$, $J_{\text{C-Pt}} = 398 \text{ Hz}$). The methoxyoxalyl derivatives are distinguishable from other α -ketoacyl complexes in several respects. Complexes **13d**–**15d** are yellow. Indeed, their MLCT bands show a blue shift of about 100 nm relative to those of other α -ketoacyl analogs. The IR absorptions of the β -CO of the methoxyoxalyl ligands are in the region of higher wavenumbers ($> 1700 \text{ cm}^{-1}$), and the α -CO absorptions are similar to those of other α -ketoacyl ligands.

The molecular structures of **13a**, **14b,d**, **15d**, and **16c** have been determined by X-ray crystallographic analysis. The ORTEP drawings of the three representatives **14b**, **15d**, and **16c** with ellipsoids at the 20% probability level are shown in Figure 2. They have a trans square-planar geometry, and the bond parameters of $\text{trans-Pt}(\text{COCOR})(\text{R}')(\text{PPh}_3)_2$ are similar to those corresponding ones of $\text{trans-Pt}(\text{COR})(\text{R}')(\text{PPh}_3)_2$. The oxalyl moiety in **14b** or **15d** is in a planar s-trans configuration with the O1–C1–C2–O2 torsion angle being $178(2)$ or $178(2)^\circ$, respectively, and is substantially distorted from the planar mold in **16c** ($141(1)^\circ$). The oxalyl C–C bonds of the α -ketoacyl ligands are generally ca. 0.1 \AA longer than the standard $\text{C}(\text{sp}^2)\text{--C}(\text{sp}^2)$ bond (ca. 1.45 \AA).^{17,18} These data indicate that electronic delocalization in the α -ketoacyl ligands is of limited importance. The wide span of the α -ketoacyl conformation may be readily influenced by either steric or environmental conditions, such as the ligand size, crystal packing, etc.

Transpositional Isomerization of $\text{trans-Pt}(\text{COCOR})(\text{R}')(\text{PPh}_3)_2$ Leading to $\text{trans-Pt}(\text{COR})(\text{COR}')(\text{PPh}_3)_2$. A typical reaction of $\text{trans-Pt}(\text{COCOR})(\text{R}')(\text{PPh}_3)_2$, which reflects the weak oxalyl C–C bond of the α -ketoacyl ligands, is spontaneous decarbonylation of such complexes in solutions at room temperature, leading to trans diacyl complexes. As shown in Scheme 13, $\text{trans-Pt}(\text{COCOR})(\text{R}')(\text{PPh}_3)_2$ species (**13c**, **14a–c**, **15a,b**) exclusively transform to $\text{trans-Pt}(\text{COR})(\text{COR}')(\text{PPh}_3)_2$ ($\text{R} = \text{R}' = \text{Et}$ (**6b'**); $\text{R} = \text{Me}$, $\text{R}' = \text{Et}$ or $\text{R} = \text{Et}$, $\text{R}' = \text{Me}$ (**6d'**); $\text{R} = \text{Me}$, $\text{R}' = \text{Ph}$ or $\text{R} = \text{Ph}$, $\text{R}' = \text{Me}$ (**6e'**); $\text{R} = \text{Ph}$, $\text{R}' = \text{Et}$ or $\text{R} = \text{Et}$, $\text{R}' = \text{Ph}$ (**6f'**)). (Our previous attempts to prepare the trans diacyl complexes by the reactions of $\text{trans-Pt}(\text{COR})(\text{CO})(\text{PPh}_3)_2^+$ and nucleophilic reagents such as $\text{R}'\text{MgX}$ and $\text{R}'\text{Li}$ only resulted in unidentified decomposed residue.) The reactions of Scheme 13 are facile in noncoordinating solvents. Coordinating solvents such as diethyl ether, THF, acetone, acetonitrile, and water or a ligating compound such as PPh_3 severely hindered these reac-

tions to varied extents. The reaction of **15c** resulted in $\text{trans-Pt}(\text{COPh})_2(\text{PPh}_3)_2$ (**6c'**) as the major product along with unidentified side products. The products from the reactions of **13a** and **13b** were complicated, although the expected $\text{trans-Pt}(\text{COMe})_2(\text{PPh}_3)_2$ (**6a'**) and **6d'** in $< 20\%$ yields were indeed detected by NMR techniques. The reactivity shown in Scheme 13 apparently depends on the variation of R' , following the order $\text{Et} \gg \text{Ph} > \text{Me}$. Besides, when complexes have a common R' ligand, the reactivity of benzoylformyl derivatives (Pt--CO--COPh) appears to be more facile than that of the derivatives with COCOME and COCOEt .

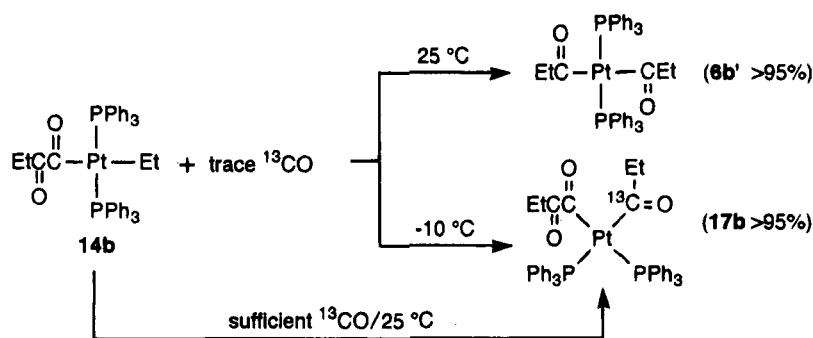
At $25 \text{ }^\circ\text{C}$ in the presence of trace ^{13}CO in CDCl_3 , exclusive transformation from **14b** to **6b'** without incorporation of ^{13}CO was still found within 1 h. However, when the reaction was carried out at $-10 \text{ }^\circ\text{C}$, a new product (designated as $^{13}\text{C-17b}$, vide supra) instead of **6b'** was acquired after 12 h. The ^{31}P NMR spectrum of $^{13}\text{C-17b}$ consists of a pair of doublets at δ 14.0 ($J_{\text{C-P}} = 112 \text{ Hz}$, $J_{\text{P-Pt}} = 1577 \text{ Hz}$) and δ 13.7 ($J_{\text{C-P}} \approx 16 \text{ Hz}$, $J_{\text{P-Pt}} = 1861 \text{ Hz}$), and its ^1H NMR spectrum has two sets of ethyl resonances at δ 2.00, 0.22 and δ 1.74, 0.68, respectively. The NMR data for $^{13}\text{C-17b}$ resemble those for the cis diacyl complex, and the incorporation of ^{13}CO completely takes place in the resulting propionyl ligand. The complex $^{13}\text{C-17b}$ is thus assigned as the novel acyl α -ketoacyl complex $\text{cis-Pt}(^{13}\text{COEt})(\text{COCOEt})(\text{PPh}_3)_2$ with the labeled CO completely incorporated in the propionyl ligand. The coexistence of **14b** and sufficient ^{13}CO in solution at $25 \text{ }^\circ\text{C}$ also afforded $^{13}\text{C-17b}$ exclusively within a few minutes. The results of the labeling experiments as shown in Scheme 14 strongly support that the reactions of Scheme 13 are intramolecular and that the carbonylation of **14b** is intermolecular.

The alkyl (or aryl) methoxyoxalyl derivatives $\text{trans-Pt}(\text{COCO}_2\text{Me})(\text{R}')(\text{PPh}_3)_2$ follow a reaction pattern different from that of other α -ketoacyl analogs. Heating $\text{trans-Pt}(\text{COCO}_2\text{Me})(\text{Me})(\text{PPh}_3)_2$ (**13d**) at $65 \text{ }^\circ\text{C}$ for 5 min first resulted in $\text{cis-Pt}(\text{CO}_2\text{Me})(\text{Me})(\text{PPh}_3)_2$ (**2f**) in $> 90\%$ yield. Complex **2f** then suffered displacement of PPh_3 by CO, yielding (*SP-4-2*)- and (*SP-4-4*)- $\text{Pt}(\text{PPh}_3)(\text{CO}_2\text{Me})(\text{CO})(\text{Me})$ (**8b** and **8b'**).¹⁹ At $45 \text{ }^\circ\text{C}$ in d_6 -acetone, complex **14d** decomposed to $\text{cis-Pt}(\text{CO}_2\text{Me})(\text{Et})(\text{PPh}_3)_2$ (**3f**) in 30% conversion within 10 min. After 30 min, the starting **14d** completely disappeared, and complex **3f** and the new compound $\text{cis-Pt}(\text{COCO}_2\text{Me})(\text{COEt})(\text{PPh}_3)_2$ (**17d**) in the ratio 1.2:1 were found. The latter product was apparently formed via facile carbonylation of **14d**. The incorporated CO has to be released from $-\text{COCO}_2\text{Me}$ of **14d** during the formation of **3f**. Complex **3f** was isolated by recrystallization from acetonitrile. Complex **3f** undergoes substitution of CO for a PPh_3 ligand to form (*SP-4-2*)- and (*SP-4-4*)- $\text{Pt}(\text{PPh}_3)(\text{CO}_2\text{Me})(\text{CO})(\text{Et})$ (**8c** and **8c'**) in the ratio 2.6:1 with 60% conversion (Scheme 15). The rest of **3f** decomposed, and identification of the residue was not attempted.

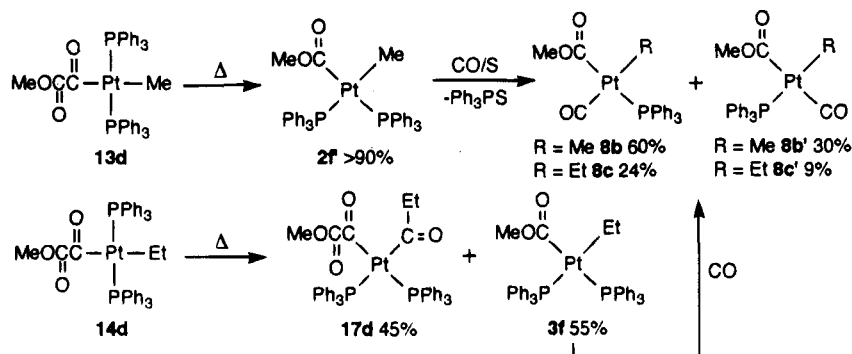
Formation of $\text{cis-Pt}(\text{COCOR})(\text{COR}')(\text{PPh}_3)_2$ via Carbonylation of $\text{trans-Pt}(\text{R}')(\text{COCOR})(\text{PPh}_3)_2$. Reactions of $\text{trans-Pt}(\text{COCOR})(\text{R}')(\text{PPh}_3)_2$ ($\text{R}' = \text{Et}$, $\text{R} = \text{Me}$, Et , Ph , OMe (**14a–d**); $\text{R}' = \text{Ph}$, $\text{R} = \text{Me}$, Et , Ph , OMe (**15a–d**)) with CO readily provided the bright yellow acyl α -ketoacyl complexes $\text{cis-Pt}(\text{COCOR})(\text{COR}')(\text{PPh}_3)_2$ ($\text{R}' = \text{Et}$, $\text{R} = \text{Me}$, Et , Ph , OMe (**17a–d**); $\text{R}' = \text{Ph}$, $\text{R} = \text{Me}$,

(18) Chen, J.-T. *J. Chin. Chem. Soc.* **1992**, *39*, 603.(19) Hsu, B.-C.; Huang, T.-M.; Chen, J.-T.; Cheng, M.-C.; Lee, G.-H.; Wang, Y. *J. Chin. Chem. Soc.*, in press.

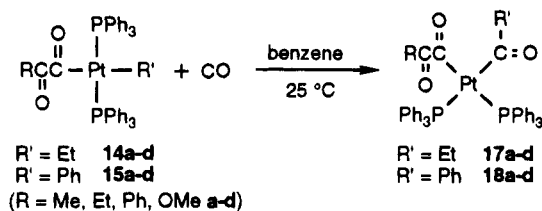
Scheme 14



Scheme 15



Scheme 16



Et, Ph, OMe (**18a-d**)) (Scheme 16). Further exposure to CO at 1 atm did not cause any change to the acyl α -ketoacyl products. The carbonylation of ethyl complexes **14a-d** (ca. 20 mg and monitored by NMR) at $0\text{ }^\circ\text{C}$ in CO -saturated chloroform is quantitative, and the reactions could be done within 1 h. It took over 1 day for the phenyl derivatives to finish the reactant under the same conditions. During the long course of carbonylation of complexes **15a-d**, the products of cis benzoyl α -ketoacyl complexes have already started to decompose (vide supra). The carbonylation of methyl derivatives could be observed in benzene, but the reactions were far from completion. The acetylide derivatives have never been detected under atmospheric pressure of CO . Adding PPh_3 to the systems and decreasing the concentration of CO have markedly retarded such carbonylation.

The NMR data for the new cis acyl α -ketoacyl complexes are similar to those for the cis diacyl complexes. In the infrared spectra of **17** and **18**, three prominent carbonyl bands could be clearly identified. The MLCT bands are generally (30–50 nm) lower than those of trans alkyl α -ketoacyl complexes. The X-ray structures of **17a** and **18a** have been obtained and are shown in parts b and c of Figure 3, respectively. Like the diacyl species, the cis acyl α -ketoacyl complexes have a distorted-square-planar geometry with $\text{C-Pt-C} = 79.8(4)^\circ$ in **17a** and $78.1(4)^\circ$ in **18a**. The distance between the two α -carbon atoms is $2.63(1)\text{ \AA}$ in **17a** and

$2.55(1)\text{ \AA}$ in **18a**, which fall in the shortest realm for the nonbonded vicinal σ -hydrocarbyls.^{16a,20} Their α -ketoacyl ligands are in an *s-trans* configuration with the torsion angle O1-C1-C2-O2 being $158(1)^\circ$ in **17a** and $148(1)^\circ$ in **18a**. The $\text{Pt-C}(\alpha\text{-ketoacyl})$ bond is slightly shorter than the $\text{Pt-C}(\text{acyl})$ bond in each of the complexes. The Pt-P bond trans to the α -ketoacyl ligand is slightly longer than the one trans to the acyl ligand.

Thermolysis of *cis*-Pt(COR)(COR')(PPh₃)₂ and *cis*-Pt(COCOR)(COR')(PPh₃)₂. The aforementioned diorganoplatinum species are generally subjected to thermolysis mainly via reductive coupling of the two organic ligands. Specifically, ketone formation was obtained from trans acyl alkyl or trans acyl aryl complexes; cis diacyl complexes tend to decompose to both ketone and diketone with the former as the major product. However, when sufficient CO was applied, diketones became predominant. The decomposition of **6d** resulted in crossover ketones and diketones. The relative yields of the organic products from various diacyl complexes are collected in Table 1. Facile decarbonylation of the α -ketoacyl group and the strong Pt-C bonds in the cis acyl α -ketoacyl complexes make our attempts at "triply carbonylative" coupling unfeasible. Thermolysis of **17a** in the presence of CO at $66\text{ }^\circ\text{C}$ gave a result comparable to the reaction of **6d**, also listed in Table 1.

Detailed NMR investigation indicates that *cis*-Pt-(COCOR)(COR')(PPh₃)₂ species (**17a-c**, **18a-c**) are subjected to exclusive decarbonylation, first yielding the trans diacyl complexes **6b'-f** quantitatively (Scheme 17). Such a reaction affords a pragmatic route for the synthesis of **6c'**, since it could not be satisfactorily obtained from **15c**. The presence of excess PPh_3 significantly suppressed such processes. When the reac-

(20) Protasiewicz, J. D.; Masschelein, A.; Lippard, S. L. *J. Am. Chem. Soc.* **1993**, *115*, 809.

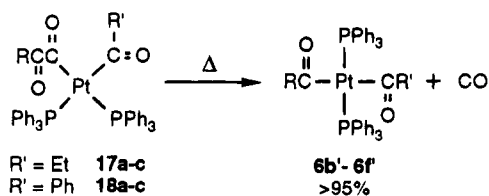
Table 1. Relative Abundance of Organic Products^a from Thermally Decomposed *cis*-Pt(COR)(COR')(PPh₃)₂^b and *cis*-Pt(COEt)(COCOMe)(PPh₃)₂^c

complex	R	R'	RC(O)R'	RC(O)C(O)R'
6a	Me	Me	35 (21) ^d	15 (60) ^d
6b	Et	Et	45 (0)	21 (100)
6d	Me	Et	— (0)	— (60)
	Me	Me	— (0)	— (20)
	Et	Et	— (0)	— (18)
6e	Me	Ph	86 (25)	14 (75)
6f	Et	Ph	100 (0)	0 (100)
17a	Me	Et	— (7.3)	— (55)
	Me	Me	— (2.4)	— (11)
	Et	Et	— (2.4)	— (15)

^a All data are based on the integration data of ¹H NMR spectra.

^b Reactions were carried out in *d*₆-benzene at 50 °C. ^c Reaction was carried out in *d*₆-benzene at 66 °C. ^d Data in parentheses were obtained from the reactions in the presence of saturated CO.

Scheme 17



tion solution was exposed to air, the *trans* diacyl complexes would further decompose to the acyl carboxylato complexes. In a typical case, when **17a** was dissolved in undried *d*₆-benzene, exclusive transformation from **17a** to **6d'** was completed after 1 day according to NMR spectroscopy. A few days later, two singlets at δ 19.48 ($J_{\text{P-Pt}} = 3655$ Hz) and 19.55 ($J_{\text{P-Pt}} = 3655$ Hz) in the ³¹P NMR spectrum increased slowly at the expense of **6d'**. In the ¹H NMR spectrum, the corresponding growing resonances were observed at δ 0.24 (t, 3H, $J_{\text{H-H}} = 7.2$ Hz), 1.25 (s, 3H), and 1.80 (q, 2H, $J_{\text{H-H}} = 7.2$ Hz) and at δ 0.66 (t, 3H, $J_{\text{H-H}} = 7.4$ Hz), 1.40 (s, 3H), 1.51 (q, 2H, $J_{\text{H-H}} = 7.4$ Hz), which have been identified as *trans*-Pt(COMe)(OCOEt)(PPh₃)₂ (**19d**) and *trans*-Pt(COEt)(OCOMe)(PPh₃)₂ (**19d'**), respectively. The relative abundances of **19d** and **19d'** were roughly 1:1, and total conversion from **17a** was 50%. In a labeling experiment, the reaction of **14c** with ¹³CO forms *cis*-Pt(¹³COEt)(COCOPh)(PPh₃)₂ (¹³C-**17c**), which spontaneously transforms to *trans*-Pt(¹³COEt)(COPh)(PPh₃)₂ (¹³C-**6f'**) via decarbonylation of the benzoyl-formyl group. Then, *trans*-Pt(¹³COEt)(OCOPh)(PPh₃)₂ (¹³C-**19f**) and *trans*-Pt(O¹³COEt)(COPh)(PPh₃)₂ (¹³C-**19f'**) were detected (Scheme 18).

The reaction starting directly from **6d'** (in other words, without the presence of CO) gave the same results. Under ambient conditions, *trans* diacyl complexes slowly transform to mixed *trans* acyl carboxylato complexes: *trans*-Pt(COR)(OCOR')(PPh₃)₂ or *trans*-Pt(OCOR)(COR')(PPh₃)₂ (R = R' = Me (**19a**), Et (**19b**), Ph (**19c**); R = Me, R' = Et (**19d**); R = Et, R' = Me (**19d'**); R = Me, R' = Ph (**19e**); R = Ph, R' = Me (**19e'**); R = Et, R' = Ph (**19f**); R = Ph, R' = Et (**19f'**)) (Scheme 19). When halogenated solvent (CHCl₃ or CH₂Cl₂) was used, *trans*-Pt(COR)(Cl)(PPh₃)₂ and *trans*-Pt(COR')(Cl)(PPh₃)₂ were the major products. The carboxylato products became the minor ones. Organic ketone was detected as well, however, only in a small quantity. When the *trans* diacyl complexes were kept under a dry nitrogen atmosphere, ketone was the major product along with

many unidentified inorganic species. In any event, no carboxylato complex was detected in such cases.

Platinum(II) complexes with hard oxygen-donor ligands are relatively rare.^{17,21} The single-crystal X-ray structure of complex **19b** has been determined and constitutes the first example of a structurally characterized platinum acyl carboxylato species, although a perfluoro analog is known.²² As is shown in the ORTEP picture in Figure 4, complex **19b** has a *trans* square-planar configuration. The carboxylato ligand is in an oxygen-bound monodentate mode. The metal-bound O1–C1 bond is slightly longer than the metal-detached O2–C1 bond (1.279(7) and 1.230(8) Å, respectively). Oxygen-donor ligands are usually weakly bonded to the Pt(II) center. Indeed, the Pt–O1 bond is 2.142(4) Å. The Pt–C4 bond (1.989 Å) *trans* to the carboxylato ligand is thus shorter than the Pt–C(acyl) bond in *trans*-Pt(COR)(R')(PPh₃)₂ or other acylplatinum complexes. The carboxylato plane Pt–O1–C1 forms a dihedral angle of 68.2(4)° with the molecular plane P1–O1–P2–C4. The angle between the acyl plane Pt–C4–O3 and the molecular plane is 98.0(6)°, again being close to a vertical feature. The torsion angle O3–C4–O1–C1 is thus 29.8(7)°.

Discussion

Transmetalation of Organoplatinum with Diorganozincs. Alkylation of platinum complexes via transmetalation has been one of the most extensively used strategic methods to prepare organoplatinum species.²³ The nucleophilic alkylating reagents employed for such a purpose comprise a wide domain of organometallics, including the Grignard reagents, organolithium, and reagents containing other main-group metals such as Hg, Cu, Cd, Tl, Sn, etc.^{1b} Curiously, the use of diorganozinc reagents for such a purpose has been uncommon. The convenient and efficient synthesis of the new *trans* alkyl (aryl) acyl and *trans* alkyl (aryl) α -ketoacyl complexes of platinum(II) with use of diorganozinc compounds provides a pragmatic extension for the usage of the transmetalation reactions of organoplatinum.

When the Grignard reagents and organolithium were used, the desired diorganoplatinum products were recovered along with significant amounts of dihaloplatinum(II) and Pt(0) residue, which caused severe problems in separation. It seemed that mild reagents for alkylation and reduction could be more appropriate. On the other hand, neither organomercury nor organotin species show any reactivity with complexes **1a–c** at ambient temperature. Increased temperature had enhanced the decarbonylation rate of the starting acylplatinum, and failed alkylation. Our survey ended with the satisfactory employment of diorganozincs. The

(21) (a) Hartley, F. R. *Chem. Rev.* **1973**, *73*, 163. (b) Hartley, F. R.; Davies, J. A. *Rev. Inorg. Chem.* **1982**, *4*, 27. (c) Davies, J. A.; Hartley, F. R. *Chem. Rev.* **1981**, *81*, 79. (d) Davis, J. A.; Hartley, F. R.; Murray, S. G. *Inorg. Chem.* **1980**, *19*, 2299. (e) Bryndza, H. E.; Tam, W. *Chem. Rev.* **1988**, *88*, 1163. (f) Siedle, A. R.; Gleason, W. B.; Newmark, R. A.; Pignolet, L. H. *Organometallics* **1986**, *5*, 1969. (g) Siedle, A. R.; Newmark, R. A.; Gleason, W. B. *J. Am. Chem. Soc.* **1986**, *108*, 767. (h) Demma, A.; Lukehart, C. M.; McPhail, A. T.; McPhail, D. R. *J. Am. Chem. Soc.* **1989**, *111*, 7615. (i) Kim, Y. J.; Osakada, K.; Takenaka, A.; Yamamoto, A. *J. Am. Chem. Soc.* **1990**, *112*, 1096.

(22) Blake, D. M.; Shields, S.; Wyma, L. *Inorg. Chem.* **1974**, *13*, 1595.

(23) Hartley, F. R. *The Chemistry of Platinum and Palladium*; Applied Science: London, 1973.

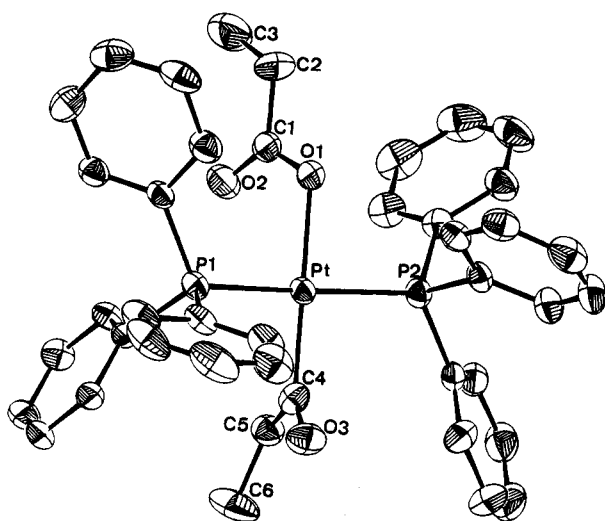
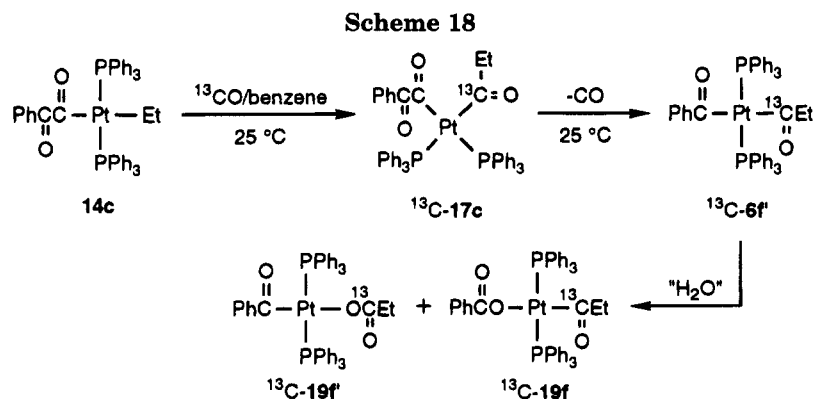


Figure 4. ORTEP drawing of *trans*-Pt(OCOEt)(COEt)(PPh₃)₂ (**19b**). (All H atoms are omitted for clarity.)

reaction conditions used for transmetalation of organohaloplatinum with R₂Zn were mild, and the yields for the desired diorganoplatinum products had been excellent. In the reactions of *trans*-Pt(COR)(X)(PPh₃)₂ or *trans*-Pt(COCOR)(L)(PPh₃)₂⁺ with R'₂Zn, *trans* diorganoderivatives result nearly quantitatively. However, in the reaction of *trans*-Pt(R)(X)(PPh₃)₂ with R'₂Zn, *cis*-Pt-(R)(R')(PPh₃)₂ becomes the predominant product.¹⁹ The stereochemical discrepancy is presumably not simply due to thermodynamic factors, since both *trans* and *cis* diorganoplatinum isomers exist. Further research is still needed to acquire kinetic rationales.

Trans Influence of α -Ketoacyl Ligands. ³¹P NMR spectroscopy affords a powerful tool for structural characterization of the diorganoplatinum(II) species. The phosphorus–platinum coupling is assumed to be dominated by the Fermi contact term and is suitable

for probing the strength of the Pt–P bond.⁸ In a pragmatic sense, the value of ¹J_{P–Pt} with respect to a phosphino ligand is sensitive to its *trans* ligand. In comparable chemical environments, the greater value of ¹J_{P–Pt} reflects a stronger P–Pt bond, thus indicating a smaller *trans* influence applied to this phosphine by its *trans* ligand. Bennett and his associates have measured the value of ¹J_{P–Pt} for Pt(Me)(L)(dppe) (dppe = bis(diphenylphosphino)ethane), in which L represents a ligand with a σ -carbon donor, to correlate ¹J_{P–Pt} with the *trans* influence of L. The results assert that the alkyl, aryl, and acyl groups are all in the category of strong *trans* influence and follow the order C(O)C₆H₉ > C₆H₉ \approx Et > Ph > CH₂Ph \approx Me.²⁴

The synthesis of *cis* acyl α -ketoacyl complexes provides new examples of organic ligands with strong *trans* influence. In *cis*-Pt(COCOR)(COR')(PPh₃)₂, the PPh₃ *trans* to the acyl ligand always has a smaller ¹J_{P–Pt} value than that of PPh₃ *trans* to an α -ketoacyl ligand (Table 2). Such data suggest that the α -ketoacyls generally have a smaller *trans* influence than the acyls but a larger influence than the aryl and the alkyl groups. Meanwhile, the length of the P–Pt bond *trans* to the α -ketoacyl group is indeed slightly shorter than that *trans* to the acyl ligand in the structures of **17a,d** and **18a**. An extended list for some σ -hydrocarbyls with decreasing *trans* influence is thus arranged as C(O)Et > C(O)Me > C(O)Ph > Et \approx COEt, COCOMe, COCOPh > Ph > COCO₂Me > CO₂Me > Me.

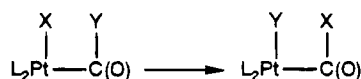
Mechanism and Reactivity of Transpositional Isomerism of *trans*-Pt(COR)(R')(PPh₃)₂ and *trans*-Pt(COCOR)(R')(PPh₃)₂. One may conceive that the reactions in both Schemes 5 and 13 result in two groups transposing between the adjacent Pt and C atoms:

(24) (a) Appleton, T. G.; Bennett, M. A. *Inorg. Chem.* **1978**, *17*, 738.
 (b) Bennett, M. A.; Rokicki, A. *J. Organomet. Chem.* **1983**, *244*, C31.
 (c) Bennett, M. A.; Rokicki, A. *Organometallics* **1985**, *4*, 180.

Table 2. ^{31}P NMR Data for *cis*-Pt(R)(R')(PPh₃)₂

complex	R	R'	$\delta(\text{P}_R)$ ($J_{\text{P-Pt}}$, Hz)	$\delta(\text{P}_{R'})$ ($J_{\text{P-Pt}}$, Hz)
2c'	Me	COPh	24.4 (2196)	20.0 (1423)
2f'	Me	CO ₂ Me	22.5 (1987)	21.4 (1879)
3f'	Et	CO ₂ Me	22.6 (1987)	21.4 (1770)
6a	C(O)Me	C(O)Me	14.0 (1558) ^a	
6b	C(O)Et	C(O)Et	14.9 (1568)	
6c	C(O)Ph	C(O)Ph	14.1 (1600) ^a	
6d	C(O)Me	C(O)Et	13.2 (1517)	14.8 (1582)
6e	C(O)Me	C(O)Ph	13.9 (1676)	15.5 (1568)
6f	C(O)Et	C(O)Ph	14.9 (1695)	15.3 (1516)
6g	C(O)C ₃ H ₅	C(O)Ph	14.7 (1598)	14.3 (1652)
6h	C(O) ⁿ Bu	C(O)Ph	15.4 (1520)	14.2 (1690)
17a	C(O)C(O)Me	C(O)Et	14.1 (1877)	14.3 (1571)
17b	C(O)C(O)Et	C(O)Et	13.7 (1861)	14.0 (1577)
17c	C(O)C(O)Ph	C(O)Et	14.8 (1860)	14.1 (1571)
17d	C(O)CO ₂ Me	C(O)Et	14.0 (1949)	14.3 (1533)
18a	C(O)C(O)Me	C(O)Ph	14.0 (1804)	14.7 (1702)
18b	C(O)C(O)Et	C(O)Ph	13.6 (1786)	14.9 (1706)
18c	C(O)C(O)Ph	C(O)Ph	14.3 (1786)	15.8 (1691)
18d	C(O)CO ₂ Me	C(O)Ph	13.7 (1882)	14.2 (1646)

^a Data were measured in *d*₆-benzene.



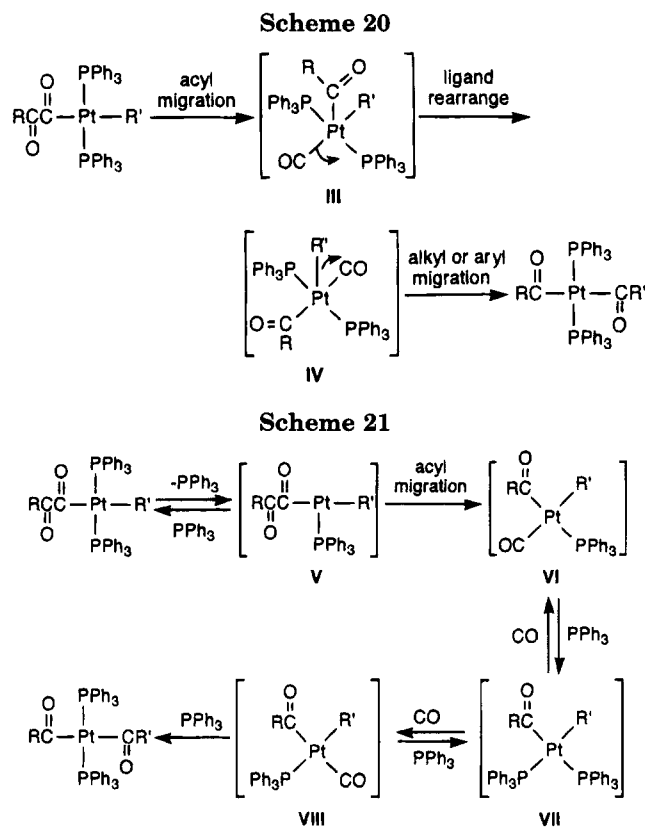
case I: X, Y = alkyl or aryl

case II: X = alkyl or aryl, Y = acyl

In the case of *trans* acyl alkyl (or aryl) complexes, two alkyl (or aryl) groups exchange to give another acyl alkyl isomer. In Scheme 13, an alkyl (or aryl) ligand switches with an acyl fragment of the α -ketoacyl ligand in *trans*-Pt(COCOR)(R')(PPh₃)₂ to give *trans*-Pt(COR)(COR')(PPh₃)₂. These two types of isomerization are unprecedented for square-planar platinum(II) systems. We name it transpositional isomerism.

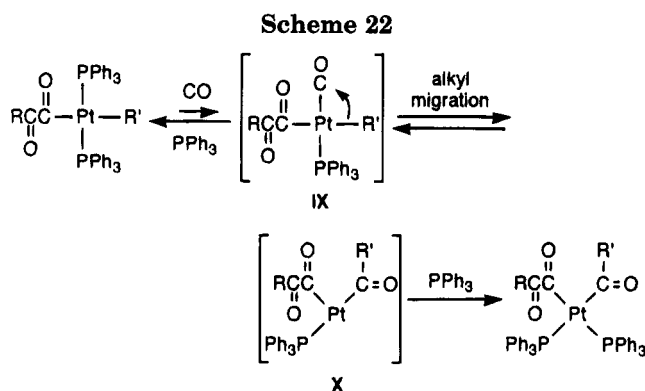
From a mechanistic point of view, since there is no incorporation of external CO in both reactions, they may comprise an intramolecular CO transfer between two *trans* organic ligands. Using the reaction of the alkyl α -ketoacyl derivative as an illustrative example, a consecutive mechanism is depicted in Scheme 20. The reaction may be preceded by decarbonylation of the α -ketoacyl ligand via an acyl migration from ligand to metal, first resulting in the five-coordinate intermediate **III**, which contains an acyl, an alkyl, and a carbonyl ligand on the same metal. The subsequent processes will comprise ligand rearrangement. The alkyl and the carbonyl ligands require *cis* positions, so that they will be available for migratory CO insertion. For example, the intermediate **IV** may be attained simply by moving the carbonyl in **III** by 90° to the vacant site. It then will constitute a good candidate for the ensuing CO insertion to finish the formation of the *trans* diacyl product. Pathways involving other unraveled five-coordinate isomerization are possible, although they may be more complicated.

Recalling that such isomerization reactions could be hindered by coordinating species, we must consider a dissociative mechanism involving four-coordinate isomerization (Scheme 21). In such a pathway, the dissociation of PPh₃ from the starting reactant first opens a coordination site (as in **V**), and facilitates the migration of the acyl group from the α -ketoacyl moiety to the metal. The four-coordinate intermediate **VI**, in which the alkyl and the carbonyl ligands are in a *trans* disposition, results. Successive ligand substitutions lead to intermediate **VII**



and then **VIII**, which contains the alkyl group and the carbonyl in *cis* positions. The alkyl migration in **VIII** and entering of the PPh₃ group will result in the *trans* diacyl complex. There are at least three reasons against this mechanism. First of all, the formation of **VIII** from **VII** by ligand substitution would allow the incorporation of external CO into the products, which is not the case. Second, intermediates **VI**–**VIII** are known to be stable species. However, none of them have been detected throughout the course of the reactions. The most critical disproof of Scheme 21 is that carbonylation does not occur for *cis*-Pt(COPh)(Me)(PPh₃)₂ (**2c'**), (*SP*-4-3)- and (*SP*-4-4)-Pt(PPh₃)(CO)(COPh)(Me) (**8a** and **8a'**), and the related species (Scheme 15).¹⁹

Mechanism and Reactivity of Stereoselective Carbonylation. The reactions of *trans* square-planar diorganoplatinum(II) complexes with carbon monoxide, leading to the *cis* carbonylated derivatives, are facile under mild conditions (Scheme 7 or 16). The stereoselectivity and reactivity of such a unique transformation are peculiarly intriguing. Our preliminary mechanistic studies on the carbonylation of both *trans*-Pt(COR)(R')(PPh₃)₂ and *trans*-Pt(COCOR)(R')(PPh₃)₂ showed that the externally provided CO had been specifically incorporated into the alkyl (or aryl) ligand. Besides, decreasing the concentration of CO and adding PPh₃ into the system severely hindered the carbonylation. Such observations may be explained by the mechanism shown in Scheme 22, in which the case of an α -ketoacyl derivative is again used for representation. Reversible substitution of CO for a PPh₃ ligand first results in the intermediate **IX**, in which the alkyl ligand is *trans* to the α -ketoacyl of strong *trans* influence and possesses the insertion-preferred *cis*-to-CO arrangement. The ensuing alkyl migration from metal to the carbon atom of the terminal carbonyl establishes the *cis* acyl α -ketoacyl structure (as in **X**). The succeeding occupancy



of the vacant coordination site by PPh_3 thus accomplishes the reaction. Since the intermediate **IX** has never been detected in any case, such a mechanism presumably follows a steady-state condition. Scheme 22 is consistent with the mechanism proposed for the diorganopalladium-mediated carbonylation reactions by Yamamoto.^{4a} An alternative associative mechanism involving a five-coordinate intermediate cannot be arbitrarily excluded, although it would be difficult to elucidate the exclusive trans to cis transformation.

The reactivity of carbonylation in the trans diorganoplatinum(II) complexes follows the unusual order $\text{Et} \gg \text{Ph} > \text{Me}$. In fact, the carbonylation of *trans*-Pt(COCOR)(Me)(PPh₃)₂ by no means competes with their decarbonylation reactions, which lead to the trans diacyl derivatives. The peculiarly slow carbonylation of the methyl derivatives is ascribed to the rapid reverse migration of the methyl group from acetyl to metal in the intermediate **X**. Such an assertion is supported by the reaction mechanism of transpositional isomerization of *trans*-Pt(COR)(Et)(PPh₃)₂, in which the decarbonylation of the acyl ligand follows the order $\text{MeC(O)} > \text{PhC(O)} \gg \text{EtC(O)}$. Consequently, the acetyl derivative **3a** readily transforms to **2b**. The analogous reactivity of the benzoyl derivative **3c** (converting to **4b**) is much lower, and none of the propionyl complexes (**2b**, **3b**, or **4b**) exhibit any activity to this kind of isomerization at all. A similar stability of the propionyl group to decarbonylation has been also observed in other systems and was attributed to the electron-releasing character of the ethyl moiety.²⁵

In contrast to the trans diorganoplatinum(II), treatment of cis acyl alkyl complexes with CO only leads to ligand substitution instead of carbonylation. For instance, the reaction of CO with *cis*-Pt(COPh)(Me)(PPh₃)₂ (**2c'**) gives (*SP*-4-3)- and (*SP*-4-4)-Pt(PPh₃)(CO)(COPh)(Me) (**8a** and **8a'**). It is worth noting that the methyl group in **8a'** is cis to the carbonyl and trans to a PPh₃ that has high trans influence. Carbonylation of **8a'** to form *trans*-Pt(COPh)(COMe)(PPh₃)₂ (**6e'**) is thought to be a legitimate reaction. In addition, **6e'** has been proved to be a thermodynamically stable species. To our surprise, CO insertion has never occurred for **8a'**. To explain the distinct reactivities of the acyl analog of **IX**, (*SP*-4-2)-Pt(PPh₃)(CO)(COPh)(Me), and **8a'** toward carbonylation, further investigation is needed.

Formation of a Cis Diacyl Complex via Addition of a Carbonucleophile to *cis*-[Pt(COPh)(CO)(P-

Ph₃)₂]⁺. There are three known electrophilic sites in *cis*-[Pt(COPh)(CO)(PPh₃)₂]⁺ (**7**): the two metal-bound carbon atoms and the platinum(II) center. It has been found that complex **7** undergoes addition of hard nucleophiles such as alkoxides or amides to result in *cis*-Pt(COPh)(CONu)(PPh₃)₂ as the only product, presumably via nucleophilic attack at the carbon of the terminal CO.^{16,26} The reaction of **7** with LiMe without external addition of CO distinguishably yields **6e**, **2c'**, and **8a**. Although the transformation between **2c'** and **8a** may take place via ligand substitution, either **2c'** or **8a** has to be first formed from the reaction of Scheme 11. Seeing that the formation of **8a'** has never been established in this reaction and that the conversion between **6e** and **2c'** has been disproved by an independent direct approach, we propose a concerted mechanism for the reaction of **7** with MeLi. The crucial addition of the carbonucleophile presumably occurs at the Pt(II) center, forming the five-coordinate intermediate **XI** (Scheme 23). Different inorganic products then may be obtained from **XI** through the independent pathways. The methyl migration from metal to CO would lead to **6e**. The loss of CO in **XI** would afford **2c'**. Complexes **8a** can result from the dissociation of the PPh₃ that is trans to CO. Departure of another PPh₃ in **XI** would produce a benzoyl methyl derivative of **IX** that could transform to **6e** according to Scheme 23. However, the facile reverse methyl migration from the resulting acetyl to metal will probably diminish the opportunity of formation of **6e** via this route.

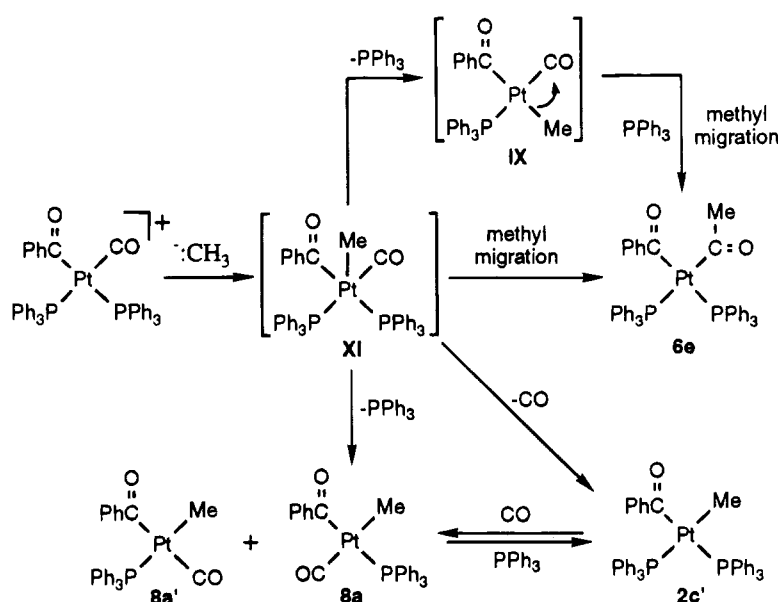
It may be interesting to take a further look into the mechanisms of certain aforementioned carbonylation or decarbonylation reactions of diorganoplatinum(II) and their intermediates. As summarized in Scheme 24, a five-coordinate intermediate in the form of **XII** was detected in the carbonylation reaction of *trans*-Pt(R)(X)L₂. The stereochemistry has been retained from the alkylhalo complex to the acylhalo product as in case A.^{2e} The other two five-coordinate intermediates **XI** and **IV** in cases B and C are isomers. They undergo migratory CO insertion, leading to the diacyl products of distinct geometry; however, both retain their stereochemistry. Case D comprises the four-coordinate intermediate **IX**. It leads to the carbonylated product with exclusive cis stereoselectivity, different from the trans reactant.

Five-coordinate species have been widely invoked in the carbonylation reactions of group 10 metal complexes,² and intramolecular isomerization of such species is generally thought to be feasible.²⁷ Those reactions containing five-coordinate intermediates in Scheme 24 seem likely to hold their geometrical character. It is possible that the energetic requirement for the migratory CO insertion (or deinsertion) in these five-coordinate species is less critical than that for isomerization, particularly with the bulky tertiary phosphines. The intermolecular processes of ligand substitution through four-coordinate species are possibly kinetically favored for the geometrical change of phosphines, compared to the case for the five-coordinate systems. One should not overinterpret the significance of Scheme 24, though, since most of these intermediate species have not been found experimentally.

(25) (a) Stille, J. K.; Regan, M. T. *J. Am. Chem. Soc.* **1974**, *96*, 1508. (b) Shie, J.-Y.; Lin, Y.-C.; Wang, Y. *J. Organomet. Chem.* **1989**, *371*, 383.

(26) (a) Huang, L.; Ozawa, F.; Yamamoto, A. *Organometallics* **1990**, *9*, 2603. (b) Shi, H.-Y. M.S. Thesis, National Taiwan University, 1993. (27) (a) Anderson, G. K.; Cross, R. *J. Chem. Soc. Rev.* **1980**, *9*, 185. (b) Cross, R. *J. Chem. Soc. Rev.* **1985**, 197.

Scheme 23



Geometrical Isomerization of $\text{Pt}(\text{CO}_2\text{Me})(\text{Me})(\text{PPh}_3)_2$. Treatment of **2f** with CO results in reversible catalytic trans-cis isomerization instead of carbonylation. The ^{13}C O-labeling experiment indicates that ^{13}C O scrambles in both cis and trans products. A reversible mechanism involving intramolecular methoxy migration in a four-coordinate intermediate is proposed as shown in Scheme 25. The intermediates **XIII** and **XIII'** are methoxycarbonyl methyl derivatives of **IX** and **VI**, respectively. In **XIII**, intramolecular transfer of the hard methoxy group between carbonyls probably overwhelms the migration of the soft methyl carbonucleophile. Other examination of the CO-promoted cis-trans isomerization of $\text{Pt}(\text{CONEt}_2)_2(\text{PPh}_3)_2$ and $\text{Pt}(\text{CONEt}_2)(\text{COCOPh})(\text{PPh}_3)_2$ indicates that they follow comparable reaction patterns.²⁶ An alternative pathway involving isomerization among five-coordinate intermediates such as **XIV** and **XIV'** ought to be as important.

C(O)-C(O) Bond Formation via Reductive Coupling of Diorgano Complexes and Decomposition of $\text{cis-Pt}(\text{COCOR})(\text{COR}')(\text{PPh}_3)_2$. The formation of ketones and vicinal diketones from diorganoplatinum(II) complexes provides the first stoichiometric examples of the palladium-mediated cross-coupling and carbonylative coupling of acid halides with organometallics (Scheme 1). The solid-state structures of cis diacyl and cis acyl α -ketoacyl complexes of platinum(II) containing extraordinarily short $\text{C}_\alpha\text{-C}_\alpha$ distances (2.5–2.7 Å), thought to potentially facilitate their bond forming. However, the strength of the Pt-C bonds and the weakness of the oxalyl C-C bonds place formation of the C(O)-C(O) bond in heavy competition with many reaction pathways such as the decarbonylation of the α -ketoacyl or acyl ligand, substitution, isomerization, etc. As indicated in Table 1, a cis diacyl complex with an acyl ligand that is stable to decarbonylation (e.g. propionyl) would have a better chance to decompose to diketones. In addition, the deliberate supply of CO would help the acyl ligand to resist decarbonylation, leading to a similar effect. In contrast, acetyl complexes that are known to be reactive to decarbonylation would tend to give ketone rather than diketone products, unless sufficient CO is provided.

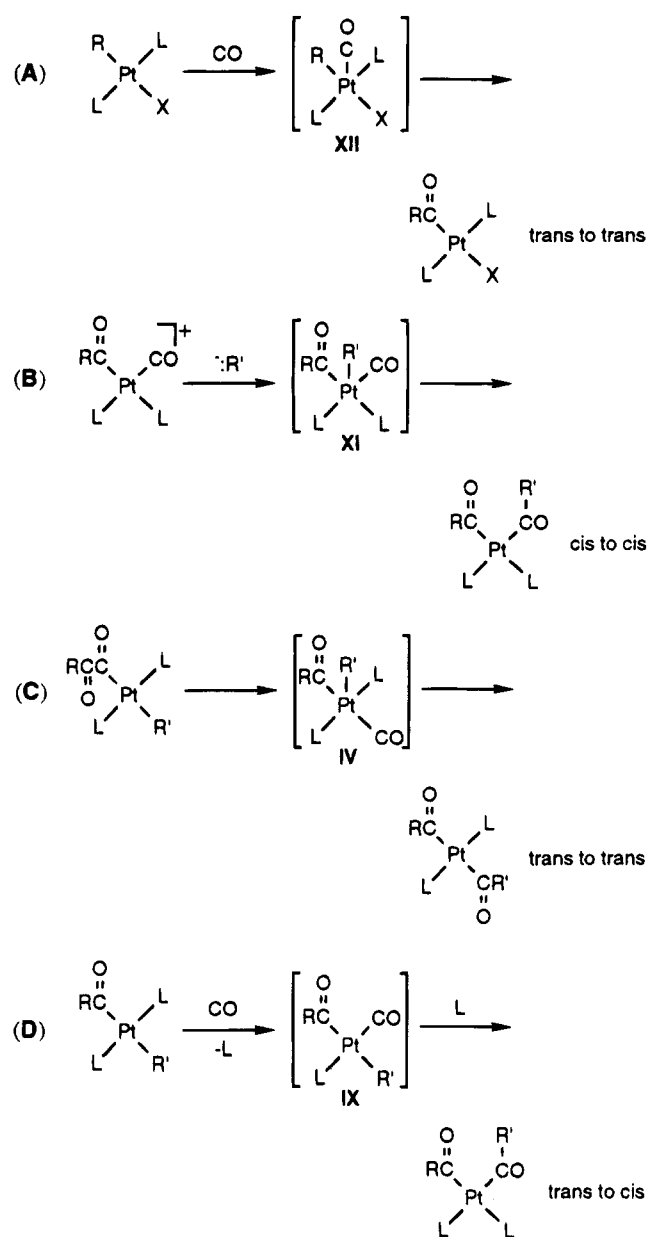
“Triple carbonylation” via reductive coupling of $\text{cis-Pt}(\text{COCOR})(\text{COR}')(\text{PPh}_3)_2$ has never succeeded. In view of the reactivity of oxalyl C-C bond cleavage in all α -ketoacyl species, this “disappointment” should not be a surprise.¹⁸ On the other hand, the stereoselective transformation of $\text{cis-Pt}(\text{COCOR})(\text{COR}')(\text{PPh}_3)_2$ to $\text{trans-Pt}(\text{COR})(\text{COR}')(\text{PPh}_3)_2$ is still unique to organoplatinum chemistry. If we recall the severe hindrance of such reactions by deliberately added PPh_3 , the dissociative mechanism of Scheme 26 provides the rationale. In $\text{cis-Pt}(\text{COR}')(\text{COCOR})(\text{PPh}_3)_2$, departure of the PPh_3 ligand cis to the α -ketoacyl group may be facilitated by the stronger trans influence of the acyl ligand, first affording the tricoordinate species **X'**. The coordinative unsaturation of **X'** promotes the decarbonylation of the α -ketoacyl ligand,¹⁶ leading to the intermediate **XV**, which has a trans diacyl framework. The rapid subsequent replacement of a PPh_3 for CO in **XV** then gives the product. The succeeding formation of the trans acyl carboxylato complexes from the trans diacyl complexes was an astonishing result. Since such reactions may be quenched by anhydrous conditions, the extra oxygen atom presumably originates from trace water in the reaction solutions.

Concluding Remarks

Compared with other organoplatinum species, the chemistry of the square-planar diorganoplatinum(II) complexes, particularly those containing acyl ligands, has been relatively less investigated.²⁸ We have successfully developed the synthesis of new trans diorganoplatinum(II) complexes such as acyl alkyl, acyl aryl, alkyl α -ketoacyl, and aryl α -ketoacyl derivatives. A pragmatic synthetic methodology has been established by applying transmetalation or alkylation with use of a diorganozinc reagent. Such trans complexes perform a series of unprecedented novel organometallic transformations involving important migratory steps of CO

(28) (a) Whitesides, G. M. *Pure Appl. Chem.* **1981**, *53*, 287. (b) McCarthy, T. T.; Nuzzo, R. G.; Whitesides, G. M. *J. Am. Chem. Soc.* **1981**, *103*, 3396, 3404. (c) Komiya, S.; Morimoto, Y.; Yamamoto, T.; Yamamoto, A. *Organometallics* **1982**, *1*, 1528.

Scheme 24



insertion and deinsertion under mild conditions. For instance, the unique stereoselective carbonylation of *trans*-Pt(COR)(R')(PPh₃)₂ and *trans*-Pt(COCOR)(R')(PPh₃)₂ leads to new square-planar *cis* diacyl and *cis* acyl α -ketoacyl complexes, respectively, in quantitative yields. *Trans* diacyl derivatives result exclusively from *trans*-Pt(COCOR)(R')(PPh₃)₂ or *cis*-Pt(COCOR)(COR')(PPh₃)₂. The stereoselectivity of these processes appears to be mainly due to kinetic rather than thermodynamic considerations. Each transformation is the outcome of competition of various fundamental steps such as functional migration, ligand substitution, isomerization, and reductive ligand coupling. Mechanistic studies implicate that those reactions with retention of geometrical integrity preferably proceed by intramolecular pathways via pentacoordinate intermediates. In contrast, those transformations with a change of geometrical configuration are likely dominated by an intermolecular avenue of ligand substitution via tetra-coordinate intermediates. This article not only reveals new scope in the realm of organoplatinum chemistry but also for the first time provides well-characterized stoi-

chiometric model examples for the palladium-mediated coupling and carbonylative coupling of acid halides and organometallics.

Experimental Section

General Considerations. Commercially available reagents were purchased and used without further purification unless otherwise indicated. Benzene, toluene, hexane, diethyl ether, and tetrahydrofuran were distilled from purple solutions of benzophenone ketyl under nitrogen, and methylene dichloride, chloroform, and acetonitrile were dried by P₂O₅ and distilled immediately prior to use. Air-sensitive material was manipulated under a nitrogen atmosphere in a glovebox or by standard Schlenk techniques. All UV-visible spectroscopic data were recorded on a Hewlett-Packard 8452A spectrophotometer. The IR spectra were recorded on a Bio-Rad FTS-40 spectrophotometer. The NMR spectra were measured on either a Bruker AC-200 or a Bruker AC-300 spectrometer. For the ³¹P NMR spectra, the spectrometer frequencies 81.015 and 121.49 MHz were employed, respectively; the corresponding frequencies for ¹³C NMR spectra were 50.324 and 75.469 MHz, respectively. The chemical shifts of ³¹P data are given in ppm (δ) relative to 85% H₃PO₄ either in CDCl₃ or in *d*₆-benzene. Values upfield of the standard are defined as negative. The chemical shifts of ¹H and ¹³C data are given in ppm (δ) relative to tetramethylsilane in CDCl₃ (δ 0.00) or to benzene in *d*₆-benzene (δ 7.15, C₆H₆; δ 128.7, C₆H₆). ¹H-coupled ¹³C NMR spectra were obtained on a Bruker AMX500 spectrometer (125.76 Hz). Mass spectrometric analyses were performed on a JEOL SX-102A spectrometer. Elemental analyses were done on a Perkin-Elmer 2400 CHN analyzer.

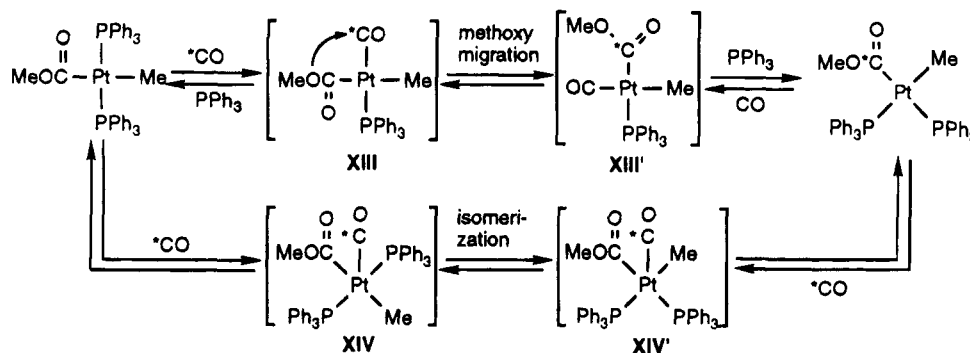
Synthesis and Characterization. *trans*-Pt(Me)(COMe)(PPh₃)₂ (**2a**). A round-bottom flask containing 220 mg (0.276 mmol) of **1a** was first charged with 20 mL of dry benzene, followed by Me₂Zn, through a cannula. After 25 min of vigorous stirring, the solution was concentrated to about 5 mL in vacuo. The addition of 5 mL of *n*-hexane first caused the precipitation of zinc salts. The yellow solid product resulted by adding a larger amount (ca. 30 mL) of *n*-hexane. The desired product was obtained by chromatographing on a silica gel column with diethyl ether and benzene (2:1 v/v) as eluent, giving 103 mg (59%) of **2a**. IR (KBr pellet): ν_{CO} 1600 cm⁻¹. ³¹P NMR (C₆D₆): δ 24.5 ($J_{\text{P-Pt}}$ = 3361 Hz). ¹H NMR (C₆D₆): δ 1.65 (3H, s, COCH₃), 0.41 (3H, t, $J_{\text{H-P}}$ = 6.8 Hz, $J_{\text{H-Pt}}$ = 42 Hz, CH₃). Anal. Calcd for PtC₃₉H₃₆OP₂: C, 60.23; H, 4.67. Found: C, 59.23; H, 4.56.

trans-Pt(Me)(COEt)(PPh₃)₂ (**2b**). Refer to **2a** for experimental details. Complex **2b** was alternatively prepared by heating **3a** (15 mg) in *d*₆-benzene at 50 °C for 2 h and then precipitated by adding hexane to the reaction solution. The isolated yield was 70% (11 mg). IR (KBr pellet): ν_{CO} 1623 cm⁻¹. ³¹P NMR (C₆D₆): δ 24.9 ($J_{\text{P-Pt}}$ = 3396 Hz). ¹H NMR (C₆D₆): δ 1.90 (2H, q, $J_{\text{H-H}}$ = 7.1 Hz, CH₂ (Et)), 0.59 (3H, t, $J_{\text{H-H}}$ = 7.1 Hz, CH₃ (Et)), 0.01 (3H, t, $J_{\text{H-P}}$ = 6.6 Hz, $J_{\text{H-Pt}}$ = 42.0 Hz, CH₃ (Me)). Anal. Calcd for C₄₀H₃₈OP₂Pt: C, 60.67; H, 4.84. Found: C, 60.04; H, 5.02.

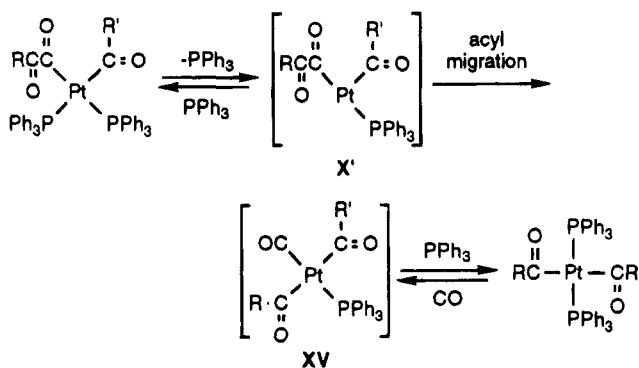
trans-Pt(Me)(COPh)(PPh₃)₂ (**2c**). Refer to **2a** for experimental details. The weight of starting **1c** was 250 mg. The isolated yield of **2c** was 135 mg (55%). IR (KBr pellet): ν_{CO} 1566 cm⁻¹. ³¹P NMR (CDCl₃): δ 26.6 ($J_{\text{P-Pt}}$ = 3284 Hz). ¹H NMR (CDCl₃): δ -0.48 (t, $J_{\text{H-P}}$ = 6.7 Hz, $J_{\text{H-Pt}}$ = 44 Hz, CH₃). ¹³C NMR (CDCl₃): δ -6.69 (t, $J_{\text{C-P}}$ = 9.2 Hz, $J_{\text{C-Pt}}$ = 384.3 Hz, CH₃), 150.9 ($J_{\text{C-P}}$ unresolved, $J_{\text{C-Pt}}$ = 88.4 Hz, CCO), 262.2 (t, $J_{\text{C-P}}$ = 9.6 Hz, $J_{\text{C-Pt}}$ = 687 Hz, CO). Anal. Calcd for PtC₄₄H₃₈OP₂: C, 62.87; H, 4.56. Found: C, 62.96; H, 4.40.

trans-[Pt(Me)(CO)(PPh₃)₂](OTf) (**2e**). In a centrifuge tube was first placed 400 mg (0.45 mmol) of *trans*-Pt(Me)(I)(PPh₃)₂ (**2d**) and 125 mg (0.5 mmol) of AgOSO₂CF₃ (AgOTf) under dry nitrogen, followed by 7 mL of degassed benzene. The resulting solution was centrifuged to precipitate AgI. After the removal of AgI, the solution was bubbled with CO

Scheme 25



Scheme 26



for 2 min. A 330 mg (80% yield) amount of product was recovered by crystallization from benzene/hexane. IR (KBr pellet): ν_{CO} 2105 cm^{-1} . ^{31}P NMR (C_6D_6): δ 20.3 ($J_{\text{P-Pt}} = 2679$ Hz). ^1H NMR (C_6D_6): δ 0.53 (3H, t, $J_{\text{H-P}} = 8.2$ Hz, $J_{\text{H-Pt}} = 60.6$ Hz, CH_3).

trans-Pt(Me)(CO₂Me)(PPh₃)₂ (2f). To a solution of 15 mL of CH_2Cl_2 containing 100 mg (0.11 mmol) of *trans*-[Pt(Me)(CO)(PPh₃)₂](OTf) was added 0.2 mmol of NaOMe (in methanol) under dry nitrogen. The solution was allowed to react for 5 min. It was then concentrated to ca. 5 mL and was filtered into stirred hexane. The product was collected in 84% yield (74 mg). IR (KBr pellet): ν_{CO} 1622 cm^{-1} . ^{31}P NMR (CDCl_3): δ 25.9 ($J_{\text{P-Pt}} = 3145$ Hz). ^1H NMR (CDCl_3): δ 2.48 (3H, s, OCH_3), -0.5 (3H, t, $J_{\text{H-P}} = 6.7$ Hz, $J_{\text{H-Pt}} = 51.5$ Hz, CH_3).

trans-Pt(Me)(¹³CO₂Me)(PPh₃)₂. ^{31}P NMR (CDCl_3): δ 25.9 (d, $J_{\text{P-C}} = 12$ Hz, $J_{\text{P-Pt}} = 3128$ Hz). ^1H NMR (CDCl_3): δ 2.50 (3H, d, $J_{\text{H-C}} = 3.43$ Hz, OCH_3), -0.5 (3H, t, $J_{\text{H-P}} = 6.7$ Hz, $J_{\text{H-Pt}} = 51.5$ Hz, CH_3). ^{13}C NMR (CDCl_3): δ 209.3 (t, $J_{\text{P-C}} = 12$ Hz, $J_{\text{Pt-C}} = 891$ Hz, CO_2Me).

cis-Pt(Me)(CO₂Me)(PPh₃)₂ (2f'). A 0.5 mL amount of C_6D_6 was first saturated with CO, and then 25 mg of 2f was dissolved in it. The reaction species were identified by NMR techniques. IR (KBr pellet): ν_{CO} 1625 cm^{-1} . ^{31}P NMR (CDCl_3): δ 22.5 (d, $J_{\text{P-P}} = 14$ Hz, $J_{\text{P-Pt}} = 1987$ Hz), 21.4 (d, $J_{\text{P-P}} = 14$ Hz, $J_{\text{P-Pt}} = 1879$ Hz). ^1H NMR (CDCl_3): δ 2.96 (3H, s, $J_{\text{H-Pt}} = 6.4$ Hz, OCH_3), 0.51 (3H, dd, $J_{\text{H-P}} = 6.7$ Hz, $J_{\text{H-Pt}} = 67$ Hz, CH_3).

cis-Pt(Me)(¹³CO₂Me)(PPh₃)₂. ^{31}P NMR (CDCl_3): δ 22.7 (dd, $J_{\text{P-C}} = 12$ Hz, $J_{\text{P-P}} = 15$ Hz, $J_{\text{P-Pt}} = 1990$ Hz), 21.8 (dd, $J_{\text{P-C}} = 163$ Hz, $J_{\text{P-P}} = 15$ Hz, $J_{\text{P-Pt}} = 1906$ Hz). ^1H NMR (CDCl_3): δ 2.95 (3H, d, $J_{\text{C-H}} = 3.12$ Hz, $J_{\text{H-Pt}} = 6.4$ Hz, OCH_3). ^{13}C NMR (CDCl_3): δ 199.7 (dd, $J_{\text{P-C}} = 163, 12$ Hz, $J_{\text{C-Pt}} = 1330$ Hz, CO_2Me).

trans-Pt(Et)(COMe)(PPh₃)₃ (3a). A 200 mg (0.25 mmol) amount of 1a and 0.17 mL of ZnEt_2 reagent (1.0 M solution in hexane) was allowed to react in 10 mL of dry N_2 -degassed benzene at 25 $^\circ\text{C}$ for 20 min. The solution was concentrated in vacuo. The addition of 5 mL of hexane first caused the precipitation of white ZnCl_2 . The yellow filtrate was transferred into 30 mL of hexane, giving yellow solids. A final 58%

(115 mg) isolated yield of 3a was obtained after recrystallization from benzene/hexane. IR (KBr pellet): ν_{CO} 1597 cm^{-1} . ^{31}P NMR (C_6D_6): δ 23.6 ($J_{\text{P-Pt}} = 3472$ Hz). ^1H NMR (C_6D_6): δ 1.53 (3H, s, CH_3 (Me)), 0.85 (2H, qt, $J_{\text{H-H}} = 7.3$ Hz, $J_{\text{H-P}} = 7.6$ Hz, $J_{\text{H-Pt}} = 47.8$ Hz, CH_2 (Et)), 0.54 (3H, tt, $J_{\text{H-H}} = 7.3$ Hz, $J_{\text{H-P}} = 4.2$ Hz, $J_{\text{H-Pt}} = 22.5$ Hz, CH_3 (Et)). Anal. Calcd for $\text{C}_{40}\text{H}_{38}\text{O}_2\text{Pt}$: C, 60.67; H, 4.85. Found: C, 60.73; H, 4.94.

trans-Pt(Et)(COEt)(PPh₃)₂ (3b). Refer to 3a for experimental details. The reaction of 300 mg of 3b gave 92 mg of 3b (71%). IR (KBr pellet): ν_{CO} 1603 cm^{-1} . ^{31}P NMR (C_6D_6): δ 23.9 ($J_{\text{P-Pt}} = 3486$ Hz). ^1H NMR (C_6D_6): δ 1.89 (2H, q, $J_{\text{H-H}} = 7.1$ Hz, CH_3 (COEt)), 0.85 (2H, qt, $J_{\text{H-H}} = 7.4$ Hz, $J_{\text{H-P}} = 6.7$ Hz, $J_{\text{H-Pt}} = 45.2$ Hz, CH_2 (Et)), 0.57 (3H, t, $J_{\text{H-H}} = 7.4$ Hz, $J_{\text{H-Pt}} = 27.6$ Hz, CH_3 (Et)), 0.44 (3H, t, $J_{\text{H-H}} = 7.1$ Hz, CH_3 (COEt)). Anal. Calcd for $\text{C}_{41}\text{H}_{40}\text{O}_2\text{Pt}$: C, 61.11; H, 5.00. Found: C, 60.83; H, 4.98.

trans-Pt(Et)(COPh)(PPh₃)₂ (3c). Refer to 3a for experimental details. The reaction of 300 mg of 3b gave 225 mg of 3b (82%). IR (KBr pellet): ν_{CO} 1560 cm^{-1} . ^{31}P NMR (CDCl_3): δ 25.4 ($J_{\text{P-Pt}} = 3395$ Hz). ^1H NMR (CDCl_3): δ 0.36 (2H, qt, $J_{\text{H-H}} = 7.7$ Hz, $J_{\text{H-P}} = 7.4$ Hz, $J_{\text{H-Pt}} = 47.0$ Hz, CH_2 (Et)), 0.13 (3H, t, $J_{\text{H-H}} = 7.7$ Hz, $J_{\text{H-Pt}} = 27.0$ Hz, CH_3 (Et)). Anal. Calcd for $\text{C}_{45}\text{H}_{40}\text{O}_2\text{Pt}$: C, 63.30; H, 4.72. Found: C, 62.86; H, 4.72. Single crystals suitable for X-ray diffraction were grown from $\text{C}_6\text{H}_6/\text{Et}_2\text{O}$.

trans-[Pt(Et)(CO)(PPh₃)₂](OTf) (3e). A mixture of 256 mg of *trans*-Pt(Et)(I)(PPh₃)₂ and 126 mg (1.1 equiv) of AgOTf was charged with 20 mL of CO-saturated THF at 0 $^\circ\text{C}$. After removal of AgI precipitate by filtration, the resulting solution was concentrated. Introducing *n*-hexane into it gave 168 mg (67% yield) of white solid product. IR (KBr pellet): ν_{CO} 2109 cm^{-1} . ^{31}P NMR (C_6D_6): δ 20.7 ($J_{\text{P-Pt}} = 2850$ Hz). ^1H NMR (C_6D_6): δ 1.20 (2H, m, unresolved, CH_2), -0.03 (3H, t, $J_{\text{H-H}} = 7.7$ Hz, $J_{\text{H-Pt}} = 25$ Hz, CH_3).

trans-Pt(Et)(CO₂Me)(PPh₃)₂ (3f). Refer to 3f for experimental details, except that the reaction temperature was 0 $^\circ\text{C}$ and the yield was 67%. IR (KBr pellet): ν_{CO} 1623 cm^{-1} . ^{31}P NMR (C_6D_6): δ 23.7 ($J_{\text{P-Pt}} = 3305$ Hz). ^1H NMR (C_6D_6): δ 2.83 (3H, s, OCH_3), 0.96 (2H, q, $J_{\text{H-H}} = 7.5$ Hz, CH_2), 0.34 (3H, t, $J_{\text{H-H}} = 7.5$ Hz, CH_3 (Et)).

cis-Pt(Et)(CO₂Me)(PPh₃)₂ (3f'). A methoxide solution was prepared by dissolving 270 mg of NaOMe in 5.0 mL of methanol. To a solution of 15 mL of dry CH_2Cl_2 containing 241 mg of *trans*-[Pt(Me)(CO)(PPh₃)₂](OTf) was added 1.2 equiv of freshly prepared NaOMe at room temperature. The mixture was allowed to react for 20 min. Addition of *n*-hexane first caused the separation of NaOTf. Further addition of *n*-hexane resulted in precipitation of the desired product. Recrystallization from benzene/*n*-hexane gave 3f' in 35% yield. IR (KBr pellet): ν_{CO} 1645 cm^{-1} . ^{31}P NMR (CDCl_3): δ 22.6 (d, $J_{\text{P-P}} = 14.2$ Hz, $J_{\text{P-Pt}} = 1890$ Hz), 21.4 (d, $J_{\text{P-P}} = 14.2$ Hz, $J_{\text{P-Pt}} = 1770$ Hz). ^1H NMR (C_6D_6): δ 3.27 (3H, s, OCH_3), 1.95 (2H, m, unresolved coupling CH_2), 1.49 (3H, td, $J_{\text{H-P}} = 7.7$ Hz, $J_{\text{H-Pt}} = 75.5$ Hz, CH_3 (Et)).

trans-Pt(Ph)(COMe)(PPh₃)₂ (4a). A mixture of 1a (200 mg, 0.251 mmol) and Ph_2Zn (28 mg, 0.128 mmol) was charged

with dry N₂-degassed toluene and CH₂Cl₂ (3:1 v/v). The reaction solution was stirred at 25 °C for 20 min. Small amounts of hexane were introduced to the reaction solution to remove ZnCl₂ salts first. Further addition of larger amounts of hexane caused the crystallization of **4a**. Purification was done by chromatographing on silica gel using benzene/diethyl ether (1:2 v/v) as eluent, resulting in a yellow product in 56% yield (112 mg). IR (KBr pellet): ν_{CO} 1567 cm⁻¹. ³¹P NMR (CDCl₃): δ 16.4 (*J*_{P-Pt} = 3346 Hz). ¹H NMR (C₆D₆): δ 6.58 (2H, m, *o*-H (Ph)), 1.58 (3H, s, CH₃). Anal. Calcd for PtC₄₁H₃₈O₂P₂: C, 62.28; H, 4.41. Found: C, 62.46; H, 4.33.

trans-Pt(Ph)(COEt)(PPh₃)₂ (4b). Refer to **4a** for experimental details. The reaction of 121 mg of **1b** gave 92 mg of **4b** (92%). IR (KBr pellet): ν_{CO} 1599 cm⁻¹. ³¹P NMR (CDCl₃): δ 17.7 (*J*_{P-Pt} = 3343 Hz). ¹H NMR (CDCl₃): δ 6.47 (2H, m, *m*-H (Ph)), 6.30 (1H, m, *p*-H (Ph)), 6.24 (2H, m, *o*-H (Ph)), 1.63 (2H, q, *J*_{H-H} = 7.1 Hz, CH₂ (Et)), -0.12 (3H, t, *J*_{H-H} = 7.1 Hz, CH₃ (Et)). Single crystals suitable for X-ray diffraction were grown from C₆H₆/Et₂O.

trans-Pt(Ph)(COPh)(PPh₃)₂ (4c). Refer to **4a** for experimental details. The reaction of 84 mg of **1c** gave 64 mg of **4c** (73%). IR (KBr pellet): ν_{CO} 1563 cm⁻¹. ³¹P NMR (CDCl₃): δ 17.2 (*J*_{P-Pt} = 3263 Hz). ¹H NMR (CDCl₃): δ 6.32 (3H, m, *o,p*-H (Ph)), 6.57 (2H, m, *m*-H (Ph)). Single crystals suitable for X-ray diffraction were grown from C₆H₆/Et₂O. Anal. Calcd for C₄₉H₄₀O₂Pt: C, 65.25; H, 4.47. Found: C, 65.38; H, 4.68.

trans-Pt(CPh)(COPh)(PPh₃)₂ (5c). A solution of 20 mL of benzene containing 130 mg (0.15 mmol) of **1c** was charged with 17 μL (0.15 mmol) of phenylacetylene and 0.32 mL (3 mmol) of Et₂NH. The solution was allowed to react at 25 °C for 2 days. Yellow solid product was precipitated by adding excess hexane to the solution. The isolated yield was 82% (115 mg, 0.124 mmol). IR (KBr pellet): ν_{C=C} 2110 cm⁻¹, ν_{CO} 1606 cm⁻¹. ³¹P NMR (CDCl₃): δ 18.6 (*J*_{P-Pt} = 3097 Hz). Anal. Calcd for C₅₁H₄₀O₂Pt: C, 66.16; H, 4.35. Found: C, 66.60; H, 4.44. Single crystals suitable for X-ray diffraction were grown from C₆H₆/Et₂O.

cis-Pt(COME)₂(PPh₃)₂ (6a). Bubbling CO through a benzene solution containing 12 mg of **2a** under atmospheric pressure at 25 °C for 50 min led to the formation of **6a**. IR (KBr pellet): ν_{CO} 1608, 1631 cm⁻¹. ³¹P NMR (C₆D₆): δ 13.95 (*J*_{P-Pt} = 1558 Hz). ¹H NMR (C₆D₆): δ 2.09 (6H, *J*_{H-Pt} ≈ 14 Hz, CH₃).

cis-Pt(COEt)₂(PPh₃)₂ (6b). Bubbling CO through a benzene solution containing 50 mg of **2b** under atmospheric pressure at 25 °C for 2 min led to the formation of **6b**. Addition of hexane to the solution resulted in the crystallization of the product in 98% yield (51 mg). IR (KBr pellet): ν_{CO} 1611, 1635 cm⁻¹. ³¹P NMR (CDCl₃): δ 14.92 (*J*_{P-Pt} = 1568 Hz). ³¹P NMR (C₆D₆): δ 14.01 (*J*_{P-Pt} = 1540 Hz). ¹H NMR (CDCl₃): δ 0.34 (6H, t, *J*_{H-H} = 7.2 Hz, CH₃), 2.04 (4H, t, *J*_{H-H} = 7.2 Hz, CH₂). ¹H NMR (C₆D₆): δ 0.78 (6H, t, *J*_{H-H} = 7.2 Hz, CH₃), 2.55 (4H, t, *J*_{H-H} = 7.2 Hz, CH₂). Anal. Calcd for PtC₄₂H₄₀O₂P₂: C, 60.50; H, 4.83. Found: C, 61.08; H, 4.74.

cis-Pt(COPh)₂(PPh₃)₂ (6c). Refer to **6b** for experimental details. Alternatively, *cis*-[Pt(COPh)(CO)(PPh₃)₂](BF₄) was prepared in situ by treating 200 mg (0.23 mmol) of **9c** with an equimolar amount of AgBF₄ in CH₂Cl₂ at -29 °C. Careful control of the temperature was necessary to avoid facile isomerization of *cis*-[Pt(COPh)(CO)(PPh₃)₂](BF₄) to its thermodynamically stable *trans* isomer. After the removal of AgCl precipitate by filtration, the temperature of the solution was lowered to -63 °C, and 1.1 equiv of PhLi (as a solution in C₆H₁₂/Et₂O) was added. The reaction solution was concentrated. Solid product was obtained by adding hexane. Recrystallization in CH₂Cl₂/Et₂O afforded yellow crystals in 34% yield. IR (KBr pellet): ν_{CO} 1600, 1613 cm⁻¹. ³¹P NMR (C₆D₆): δ 14.1 (*J*_{P-Pt} = 1600 Hz). Anal. Calcd for C₅₀H₄₀O₂Pt: C, 64.58; H, 4.34. Found: C, 63.84; H, 4.31. Single crystals suitable for X-ray diffraction were grown from C₆H₆/Et₂O.

cis-Pt(COME)(COEt)(PPh₃)₂ (6d). Refer to **6f** for experimental details. Addition of extra PPh₃ (2 equiv) was applied to block acyl scrambling. IR (KBr pellet): ν_{CO} 1607, 1633 cm⁻¹. ³¹P NMR (C₆D₆): δ 14.8 (*J*_{P-P} = 17.3 Hz, *J*_{P-Pt} = 1582 Hz), 13.24 (*J*_{P-P} = 17.3 Hz, *J*_{P-Pt} = 1517 Hz). ¹H NMR (C₆D₆): δ 2.55 (2H, q, *J*_{H-H} = 7.2 Hz, CH₂), 2.10 (3H, s, COCH₃), 0.80 (3H, t, *J*_{H-H} = 7.2 Hz, CH₃ (Et)). Anal. Calcd for C₄₁H₃₈O₂Pt: C, 60.07; H, 4.68. Found: C, 60.52; H, 4.87.

cis-Pt(COME)(COPh)(PPh₃)₂ (6e). Refer to **6c** for experimental details. IR (KBr pellet): ν_{CO} 1605, 1635 cm⁻¹. ³¹P NMR (C₆D₆): δ 15.0 (*J*_{P-P} = 18.5 Hz, *J*_{P-Pt} = 1522 Hz), 13.2 (*J*_{P-P} = 18.5 Hz, *J*_{P-Pt} = 1652 Hz). ¹H NMR (C₆D₆): δ 2.03 (3H, s, COCH₃). Anal. Calcd for PtC₄₅H₃₈O₂Pt: C, 62.28; H, 4.41. Found: C, 61.78; H, 4.21.

cis-Pt(COEt)(COPh)(PPh₃)₂ (6f). Through a benzene solution containing 100 mg of **2c**, CO was bubbled under atmospheric pressure at 25 °C for 2 min. The reaction solution was concentrated in vacuo. Introduction of hexane into the solution resulted in crystallization of the yellow product in 98% yield (101 mg). The carbonylation of **4b** under the same conditions was completed after 1 h. The isolated yield of **6f** was 95%. IR (KBr pellet): ν_{CO} 1604, 1622 cm⁻¹. ³¹P NMR (CDCl₃): δ 14.9 (*J*_{P-P} = 18.5 Hz, *J*_{P-Pt} = 1695 Hz), 15.3 (*J*_{P-P} = 18.5 Hz, *J*_{P-Pt} = 1516 Hz). ¹H NMR (CDCl₃): δ 2.14 (2H, q, *J*_{H-H} = 7.1 Hz, CH₂), 0.18 (3H, t, *J*_{H-H} = 7.1 Hz, CH₃). Anal. Calcd for C₄₆H₄₀O₂Pt: C, 62.65; H, 4.57. Found: C, 62.51; H, 4.70. Single crystals suitable for X-ray diffraction were grown from C₆H₆/Et₂O.

cis-Pt(COCH₂CH₂)(COPh)(PPh₃)₂ (6g). To 158 mg (0.18 mmol) of complex **9c** and 38 mg (0.2 mmol) of AgBF₄ was added 15 mL of degassed dry CH₂Cl₂. The decarbonylation reaction was allowed to continue for 40 min at -29 °C. After the removal of AgCl precipitate by filtration, the temperature was lowered to -70 °C. An 0.11 mL portion of CH₂CHCH₂MgCl (2.0 M in THF solution) was added dropwise to the freshly formed solution of *cis*-[Pt(CO)(COPh)(PPh₃)₂](BF₄). The temperature was slowly raised to -35 °C, and the reaction solution was concentrated to ca. 5 mL. The precipitate of the salt was first isolated by adding 10 mL of ice-cooled hexane/Et₂O. The filtrate was concentrated to ca. 5 mL. Repeated recrystallization in cold CH₂Cl₂/hexane afforded the yellow product in 38% yield (59 mg). A trace of *trans*-Pt(Cl)(COPh)(PPh₃)₂ and **9c** was crystallized along with the desired compound. Further purification was not successful. IR (KBr pellet): ν_{CO} 1622, 1605 cm⁻¹. ³¹P NMR (CDCl₃): δ 14.7 (*J*_{P-P} = 18.1 Hz, *J*_{P-Pt} = 1598 Hz), 14.3 (*J*_{P-P} = 18.1 Hz, *J*_{P-Pt} = 1652 Hz). ¹H NMR (CDCl₃): δ 5.27 (1H, m, C(O)CH₂CHCH₂), 4.65, 4.45 (1H for each, d, *J*_{H-H(cis)} = 10.4 Hz, *J*_{H-H(trans)} = 17.4 Hz, C(O)CH₂CHCH₂), 2.83 (2H, d, *J*_{H-H} = 6.8 Hz, C(O)CH₂-CHCH₂).

cis-Pt(COⁿBu)(COPh)(PPh₃)₂ (6h). Refer to **6g** for experimental details. The isolated yield was 60%. IR (KBr pellet): ν_{CO} 1624, 1601 cm⁻¹. ³¹P NMR (CDCl₃): δ 15.4 (*J*_{P-P} = 19.1 Hz, *J*_{P-Pt} = 1522 Hz), 14.2 (*J*_{P-P} = 19.1 Hz, *J*_{P-Pt} = 1690 Hz). ¹H NMR (CDCl₃): δ 2.09 (2H, t, *J*_{H-H} = 7.1 Hz, CH₂(CH₂)₂Me), 0.90 (4H, m, CH₂(CH₂)₂Me), 0.53 (3H, t, *J*_{H-H} = 7.1 Hz, CH₃).

trans-Pt(COME)₂(PPh₃)₂ (6a'). Refer to **6f** for experimental details. Mixed products were recovered. The characterization of **6a'** was done by spectroscopy. IR (KBr pellet): ν_{CO} 1639, 1586 cm⁻¹. ³¹P NMR (CDCl₃): δ 15.8 (*J*_{P-P} = 3417 Hz). ¹H NMR (CDCl₃): δ 0.94 (6H, s, CH₃).

trans-Pt(COEt)₂(PPh₃)₂ (6b'). Refer to **6f** for experimental details. A reaction of 78 mg of **14b** gave 48 mg of **6b'** (61%). UV-vis (CHCl₃): λ_{max} 480 nm, ε = 181 ± 5 dm³ mol⁻¹. IR (KBr pellet): ν_{CO} 1643, 1596 cm⁻¹. ³¹P NMR (CDCl₃): δ 16.2 (*J*_{P-Pt} = 3451 Hz). ¹H NMR (CDCl₃): δ 1.36 (4H, q, *J*_{H-H} = 7.2 Hz, CH₂), -0.14 (6H, t, *J*_{H-H} = 7.2 Hz, CH₃). Anal. Calcd for PtC₄₂H₄₀O₂Pt: C, 60.50; H, 4.83. Found: C, 59.88; H, 4.89.

trans-Pt(COPh)₂(PPh₃)₂ (6c'). Refer to **6f** for experimental details. A small amount of *trans*-Pt(COPh)(Cl)(PPh₃)₂ was recovered along with the desired product, and satisfactory

purification was not achieved. UV-vis (CHCl₃): λ_{\max} 434 nm, $\epsilon = 127 \pm 5 \text{ dm}^3 \text{ mol}^{-1}$. IR (KBr pellet): ν_{CO} 1636, 1618 cm⁻¹. ³¹P NMR (CDCl₃): δ 15.4 ($J_{\text{P-Pt}} = 3404 \text{ Hz}$). ¹H NMR (CDCl₃): δ 6.8–7.8 (m, phenyl H).

trans-Pt(COMe)(COEt)(PPh₃)₂ (6d'). Refer to **6f** for experimental details. The reaction was completed within 2.5 h at 42 °C, and the yield was 68%. IR (KBr pellet): ν_{CO} 1634, 1591 cm⁻¹. ³¹P NMR (CDCl₃): δ 16.4 ($J_{\text{P-Pt}} = 3435 \text{ Hz}$). ¹H NMR (CDCl₃): δ 1.41 (2H, q, $J_{\text{H-H}} = 7.2 \text{ Hz}$, CH₂ (Et)), 0.92 (3H, s, CH₃ (Me)), -0.14 (3H, t, $J_{\text{H-H}} = 7.2 \text{ Hz}$, CH₃ (Et)). Anal. Calcd for PtC₄₁H₃₈O₂P₂: C, 60.07; H, 4.67. Found: C, 59.75; H, 4.65.

trans-Pt(COMe)(COPh)(PPh₃)₂ (6e'). Refer to **6f** for experimental details. The reaction lasted for 4 h at 25 °C, and the yield was 85%. IR (KBr pellet): ν_{CO} 1599, 1567 cm⁻¹. ³¹P NMR (CDCl₃): δ 15.4 ($J_{\text{P-Pt}} = 3371 \text{ Hz}$). ¹H NMR (CDCl₃): 0.98 (3H, s, CH₃). Anal. Calcd for PtC₄₅H₃₈O₂P₂: C, 62.28; H, 4.41. Found: C, 62.32; H, 4.40.

trans-Pt(COEt)(COPh)(PPh₃)₂ (6f). In a round-bottom flask was first placed 120 mg (0.11 mmol) of *trans*-Pt(Et)(COCOPh)(PPh₃)₂ (**14c**), followed by 12 mL of dry chloroform under nitrogen. The solution was allowed to react at 0 °C for 1 h and was then concentrated to about 2 mL in vacuo. Addition of *n*-hexane caused the precipitation of **6f**. Orange product in 89% yield (105 mg) was obtained after recrystallization from diethyl ether/*n*-hexane. Complex **6f** was alternatively prepared by decomposing **17c** (22 mg) in 0.5 mL of *d*₆-benzene at 25 °C. After 5 min, the product was precipitated by adding *n*-hexane to the reaction solution. The isolated yield was 91% (20 mg). UV-vis (CHCl₃): λ_{\max} 456 nm, $\epsilon = 141 \pm 2 \text{ dm}^3 \text{ mol}^{-1}$. IR (KBr pellet): ν_{CO} 1601, 1561 cm⁻¹. ³¹P NMR (CDCl₃): δ 16.1 ($J_{\text{P-Pt}} = 3392 \text{ Hz}$). ¹H NMR (CDCl₃): δ 1.36 (2H, q, $J_{\text{H-H}} = 7.1 \text{ Hz}$, CH₂), -0.18 (3H, t, $J_{\text{H-H}} = 7.1 \text{ Hz}$, CH₃). Anal. Calcd for PtC₄₆H₄₀O₂P₂: C, 62.65; H, 4.57. Found: C, 62.08; H, 4.63.

trans-Pt(COPh)(¹³COEt)(PPh₃)₂. ³¹P NMR (C₆D₆): δ 15.1 ($J_{\text{P-C}} = 7.7 \text{ Hz}$). ¹H NMR (C₆D₆): δ 1.85 (2H, qd, $J_{\text{H-C}} = 2.2 \text{ Hz}$, CH₂), 0.42 (3H, dt, $J_{\text{H-C}} = 4.2 \text{ Hz}$, CH₃).

(SP-4-2)-Pt(PPh₃)(CO₂Me)(CO)(Me) (8b) and (SP-4-4)-Pt(PPh₃)(CO₂Me)(CO)(Me) (8b'). Complexes **8b** and **8b'** resulted from the reaction of **2f** and CO in CDCl₃ and were characterized by NMR. **8b**: ³¹P NMR (CDCl₃) δ 20.3 ($J_{\text{P-Pt}} = 1762 \text{ Hz}$); ¹H NMR (CDCl₃) δ 3.16 (3H, s, $J_{\text{H-Pt}} = 6.2 \text{ Hz}$, OCH₃), 1.04 (3H, d, $J_{\text{H-P}} = 6.4 \text{ Hz}$, $J_{\text{H-Pt}} = 71.6 \text{ Hz}$, CH₃). **8b'**: ³¹P NMR (CDCl₃) δ 17.7 ($J_{\text{P-Pt}} = 1826 \text{ Hz}$); ¹H NMR (CDCl₃) δ 3.71 (3H, s, $J_{\text{H-Pt}} = 5.9 \text{ Hz}$, OCH₃), 0.63 (3H, d, $J_{\text{H-P}} = 9.7$, 69.6 Hz, $J_{\text{H-Pt}} = 69.6 \text{ Hz}$, CH₃).

(SP-4-2)-Pt(PPh₃)(CO₂Me)(CO)(Et) (8c) and (SP-4-4)-Pt(PPh₃)(CO₂Me)(CO)(Et) (8c'). **8c**: ³¹P NMR (CDCl₃) δ 20.3 ($J_{\text{P-Pt}} = 1762 \text{ Hz}$); ¹H NMR (CDCl₃) δ 2.48 (3H, s, OCH₃), 1.04 (3H, d, $J_{\text{H-P}} = 6.4 \text{ Hz}$, $J_{\text{H-Pt}} = 71.6 \text{ Hz}$, CH₃). **8c'**: ³¹P NMR (CDCl₃) δ 20.3 ($J_{\text{P-Pt}} = 1762 \text{ Hz}$); ¹H NMR (CDCl₃) δ 2.48 (3H, s, OCH₃), 1.04 (3H, d, $J_{\text{H-P}} = 6.4 \text{ Hz}$, $J_{\text{H-Pt}} = 71.6 \text{ Hz}$, CH₃).

trans-Pt(Cl)(COCOR)(PPh₃)₂ (R = Me, Et, Ph, OMe; 9a–d). A round-bottom flask containing 2.20 g (1.61 mmol) of Pt(PPh₃)₄ was first charged with 25 mL of dry benzene, followed by RCOCOR¹⁶ under nitrogen. After 15 min of vigorous stirring, the solution was concentrated to less than 10 mL in vacuo. Addition of 20 mL of ethanol resulted in precipitation of the desired product; 85–95% yields were usually obtained after recrystallization from *n*-hexane/diethyl ether/ethanol. **9a**: UV-vis (CH₂Cl₂) λ_{\max} 452 nm, $\epsilon = 57 \pm 2 \text{ dm}^3 \text{ mol}^{-1}$; IR (KBr pellet) ν_{CO} 1699, 1638 cm⁻¹; ³¹P NMR (CDCl₃) δ 18.2 ($J_{\text{P-Pt}} = 3256 \text{ Hz}$); ¹H NMR (CDCl₃) δ 0.87 (3H, s, CH₃); ¹³C NMR (CDCl₃) δ 214.4 ($J_{\text{C-P}} = 6.9 \text{ Hz}$, $J_{\text{C-Pt}} = 1084 \text{ Hz}$, α -CO), 200.5 ($J_{\text{C-P}} = 4.1 \text{ Hz}$, $J_{\text{C-Pt}} = 187 \text{ Hz}$, β -CO), 20.7 (CH₃). **9b**: UV-vis (CH₂Cl₂) λ_{\max} 456 nm, $\epsilon = 63 \pm 2 \text{ dm}^3 \text{ mol}^{-1}$; IR (KBr pellet) ν_{CO} 1705, 1650 cm⁻¹; ³¹P NMR (CDCl₃) δ 18.4 ($J_{\text{P-Pt}} = 3274 \text{ Hz}$); ¹H NMR (CDCl₃) δ 1.06 (2H, q, $J_{\text{H-H}} = 7.1 \text{ Hz}$, CH₂), 0.34 (3H, t, $J_{\text{H-H}} = 7.1 \text{ Hz}$, CH₃); ¹³C NMR (CDCl₃) δ 214.8 ($J_{\text{C-P}} = 6.9 \text{ Hz}$, $J_{\text{C-Pt}} = 1075 \text{ Hz}$, α -CO), 202.2

($J_{\text{C-P}} = 3.8 \text{ Hz}$, $J_{\text{C-Pt}} = 179 \text{ Hz}$, β -CO), 27.1 (CH₂), 6.9 (CH₃). **9c**: UV-vis (CH₂Cl₂) λ_{\max} 484 nm, $\epsilon = 67 \pm 2 \text{ dm}^3 \text{ mol}^{-1}$; IR (KBr pellet) ν_{CO} 1659, 1637 cm⁻¹; ³¹P NMR (CDCl₃) δ 18.9 ($J_{\text{P-Pt}} = 3284 \text{ Hz}$); ¹H NMR (CDCl₃) δ 7.3–7.8 (m, phenyl H), 6.98 (2H, m, *o*-CH (COPh)); ¹³C NMR (CDCl₃) δ 216.0 ($J_{\text{C-P}} = 6.3 \text{ Hz}$, $J_{\text{C-Pt}} = 1074 \text{ Hz}$, α -CO), 190.6 ($J_{\text{C-P}} = 3.7 \text{ Hz}$, $J_{\text{C-Pt}} = 189 \text{ Hz}$, β -CO). **9d**: UV-vis (CH₂Cl₂) λ_{\max} 378 nm, $\epsilon = 90 \pm 2 \text{ dm}^3 \text{ mol}^{-1}$; IR (KBr pellet) ν_{CO} 1726, 1708, 1654 cm⁻¹; ³¹P NMR (CDCl₃) δ 18.2 ($J_{\text{P-Pt}} = 3198 \text{ Hz}$); ¹H NMR (CDCl₃) δ 3.02 (3H, s, OCH₃); ¹³C NMR (CDCl₃) δ 208.2 ($J_{\text{C-P}} = 6.8 \text{ Hz}$, $J_{\text{C-Pt}} = 1142 \text{ Hz}$, α -CO), 163.8 ($J_{\text{C-P}} = 5.0 \text{ Hz}$, $J_{\text{C-Pt}} = 239 \text{ Hz}$, β -CO), 52.0 (OCH₃).

trans-Pt(Me)(COCOMe)(PPh₃)₂ (13a). Refer to **13d** for experimental details. The isolated yield of the purple **13a** was 25%. UV-vis (CDCl₃): λ_{\max} 536 nm, $\epsilon = 55 \pm 1 \text{ dm}^3 \text{ mol}^{-1}$. IR (KBr pellet): ν_{CO} 1698, 1604 cm⁻¹. ³¹P NMR (CDCl₃): δ 25.0 ($J_{\text{P-Pt}} = 3243 \text{ Hz}$). ¹H NMR (CDCl₃): δ 0.91 (3H, s, CH₃-CO), -0.53 (3H, t, $J_{\text{H-P}} = 6.5 \text{ Hz}$, $J_{\text{H-Pt}} = 44 \text{ Hz}$, Pt-CH₃). Anal. Calcd for PtC₄₀H₃₆O₂P₂: C, 59.63; H, 4.50. Found: C, 60.17; H, 4.61. Single crystals suitable for X-ray diffraction were grown from C₆H₆/Et₂O.

trans-Pt(Me)(COCOEt)(PPh₃)₂ (13b). Refer to **13d** for experimental details. The isolated yield for **13b** was 78%. UV-vis (CDCl₃): λ_{\max} 542 nm, $\epsilon = 52 \pm 1 \text{ dm}^3 \text{ mol}^{-1}$. IR (KBr pellet): ν_{CO} 1696, 1592 cm⁻¹. ³¹P NMR (CDCl₃): δ 25.03 ($J_{\text{P-Pt}} = 3251 \text{ Hz}$). ¹H NMR (CDCl₃): δ 1.20 (2H, q, $J_{\text{H-H}} = 7.2 \text{ Hz}$, CH₂ (Et)), 0.34 (3H, t, $J_{\text{H-H}} = 7.2 \text{ Hz}$, CH₂ (Et)), -0.53 (3H, t, $J_{\text{H-P}} = 7.0 \text{ Hz}$, $J_{\text{H-Pt}} = 45 \text{ Hz}$, CH₃ (Me)). Anal. Calcd for PtC₄₁H₃₈O₂P₂: C, 60.07; H, 4.67. Found: C, 60.40; H, 4.70.

trans-Pt(Me)(COCOPh)(PPh₃)₂ (13c). Refer to **13d** for experimental details. The isolated yield for **13c** was 51%. UV-vis (CDCl₃): λ_{\max} 548 nm, $\epsilon = 98 \pm 1 \text{ dm}^3 \text{ mol}^{-1}$. IR (KBr pellet): ν_{CO} 1667, 1578 cm⁻¹. ³¹P NMR (CDCl₃): δ 25.1 ($J_{\text{P-Pt}} = 3254 \text{ Hz}$). ¹H NMR (CDCl₃): δ -0.55 (3H, t, $J_{\text{H-P}} = 7.1 \text{ Hz}$, $J_{\text{H-Pt}} = 45 \text{ Hz}$, Pt-CH₃). Anal. Calcd for PtC₄₅H₃₈O₂P₂: C, 62.28; H, 4.41. Found: C, 62.10; H, 4.40.

trans-Pt(Me)(COCO₂Me)(PPh₃)₂ (13d). A two-neck round-bottom flask was first charged with 200 mg (0.21 mmol) of *trans*-Pt(COCOOMe)(OTf)(PPh₃)₂, followed by 10 mL of degassed dry CH₂Cl₂. At -20 °C, Me₂Zn (presumably in excess) was transferred through a cannula. Zinc salts were first removed by adding 5 mL of *n*-hexane. The addition of a larger amount (ca. 30 mL) of *n*-hexane to the solution caused the precipitation of the yellow product. Recrystallization in cold CH₂Cl₂/hexane afforded **13d** in 70% yield (120 mg). IR (KBr pellet): ν_{CO} 1705, 1615 cm⁻¹. ³¹P NMR (CDCl₃): δ 24.9 ($J_{\text{P-Pt}} = 3215 \text{ Hz}$). ¹H NMR (CDCl₃): δ 2.99 (3H, s, OCH₃), -0.50 (3H, t, $J_{\text{H-P}} = 7.1 \text{ Hz}$, $J_{\text{H-Pt}} = 45 \text{ Hz}$, Pt-CH₃). ¹³C NMR (CDCl₃): δ 237.1 ($J_{\text{C-Pt}} = 844 \text{ Hz}$, α -CO), 168.7 ($J_{\text{C-Pt}} = 129 \text{ Hz}$, β -CO), -8.6 ($J_{\text{C-P}} = 9.1 \text{ Hz}$, $J_{\text{C-Pt}} = 398 \text{ Hz}$, CH₃).

trans-Pt(Et)(COCOMe)(PPh₃)₂ (14a). Refer to **14b** for experimental details. The isolated yield for **14a** was 60–65%. UV-vis (CDCl₃): λ_{\max} 550 nm, $\epsilon = 64 \pm 1 \text{ dm}^3 \text{ mol}^{-1}$. IR (KBr pellet): ν_{CO} 1693, 1590 cm⁻¹. ³¹P NMR (CDCl₃): δ 24.6 ($J_{\text{P-Pt}} = 3363 \text{ Hz}$). ¹H NMR (CDCl₃): δ 0.86 (3H, s, CH₃), 0.36 (2H, q, $J_{\text{H-H}} = 7.4 \text{ Hz}$, $J_{\text{H-Pt}} = 48 \text{ Hz}$, CH₂ (Et)), -0.17 (3H, t, $J_{\text{H-H}} = 7.4 \text{ Hz}$, $J_{\text{H-Pt}} = 28 \text{ Hz}$, CH₃ (Et)). Anal. Calcd for PtC₄₁H₃₈O₂P₂: C, 60.07; H, 4.67. Found: C, 60.42; H, 4.67.

trans-Pt(Et)(COCOEt)(PPh₃)₂ (14b). In a round-bottom flask containing 200 mg (0.24 mmol) of **9b**, ca. 15 mL of dry benzene under nitrogen was first introduced, followed by 0.24 mL (0.24 mmol) of Et₂Zn (1 M THF solution) at 25 °C. The solution was stirred for 30 min. A 5 mL amount of ice-cooled *n*-hexane was added to precipitate zinc salts. The solution was concentrated to ca. 5 mL. The addition of 30 mL of *n*-hexane afforded purple crystalline product in 65% yield (125 mg). UV-vis (CDCl₃): λ_{\max} 552 nm, $\epsilon = 75 \pm 1 \text{ dm}^3 \text{ mol}^{-1}$. IR (KBr pellet): ν_{CO} 1696, 1604 cm⁻¹. ³¹P NMR (CDCl₃): δ 24.3 ($J_{\text{P-Pt}} = 3370 \text{ Hz}$). ¹H NMR (CDCl₃): δ 1.15 (2H, q, $J_{\text{H-H}} = 7.2 \text{ Hz}$, CH₂CH₂CO), 0.31 (3H, t, $J_{\text{H-H}} = 7.2 \text{ Hz}$, CH₃CH₂CO), 0.32 (2H, q, $J_{\text{H-H}} = 7.5 \text{ Hz}$, CH₂ (Et)), -0.15 (3H, t, $J_{\text{H-H}} = 7.5 \text{ Hz}$, CH₃ (Et)). Anal. Calcd for PtC₄₂H₄₀O₂P₂: C, 60.50; H, 4.84.

Found: C, 60.50; H, 4.83. Single crystals suitable for X-ray diffraction were grown from C_6H_6/Et_2O .

trans-Pt(Et)(COCOPh)(PPh₃)₂ (14c). [*trans*-Pt(COCOPh)(THF)(PPh₃)₂](BF₄) was first prepared *in situ*.¹¹ After the removal of AgCl by filtration, excess (>1 equiv) Et₂Zn (in *n*-hexane solution) was added to the solution. Introduction of ice-cooled *n*-hexane to the reaction solution caused the precipitation of the brown product mixture. Repeated recrystallization in THF/*n*-hexane afforded purple crystallines. After a final wash with acetone, complex **14c** was isolated in 90% yield. UV-vis (CDCl₃): λ_{max} 562 nm, ε = 142 ± 1 dm³ mol⁻¹. IR (KBr pellet): ν_{CO} 1653, 1560 cm⁻¹. ³¹P NMR (CDCl₃): δ 24.4 (*J*_{P-Pt} = 3375 Hz). ¹H NMR (CDCl₃): δ 0.29 (2H, qt, *J*_{H-H} = 7.3 Hz, *J*_{H-P} = 8.4 Hz, *J*_{H-Pt} = 28.9 Hz, CH₂), -0.32 (3H, t, *J*_{H-H} = 7.3 Hz, *J*_{H-Pt} = 25.5 Hz, CH₃). Anal. Calcd for PtC₄₆H₄₀O₂P₂: C, 62.65; H, 4.57. Found: C, 62.61; H, 4.59.

trans-Pt(Et)(COCO₂Me)(PPh₃)₂ (14d). To 10 mL of dry CH₂Cl₂ solution containing 200 mg (0.21 mmol) of *trans*-Pt(COCOME)(OTf)(PPh₃)₂ was added 0.2 mL (0.2 mmol) of Et₂Zn (1 M THF solution) at -20 °C under dry nitrogen. The mixtures were allowed to react for 30 min. The zinc salts were first removed by adding 5 mL of ice-cooled *n*-hexane. The filtrate was concentrated to ca. 5 mL. Repeated recrystallization in cold CH₂Cl₂/hexane gave yellow crystalline product in 74% yield (127 mg). UV-vis (CDCl₃): λ_{max} 452 nm, ε = 89 ± 1 dm³ mol⁻¹. IR (KBr pellet): ν_{CO} 1710, 1596 cm⁻¹. ³¹P NMR (CDCl₃): δ 24.52 (*J*_{P-Pt} = 3328 Hz). ¹H NMR (CDCl₃): δ 2.97 (3H, s, OCH₃), 0.35 (2H, qt, *J*_{H-H} = 7.4 Hz, *J*_{H-P} = 8.4 Hz, *J*_{H-Pt} = 50 Hz, CH₂), -0.05 (3H, tt, *J*_{H-H} = 7.4 Hz, *J*_{H-Pt} = 29 Hz, CH₃ (Et)). Anal. Calcd for PtC₄₁H₃₈O₃P₂: C, 58.92; H, 4.58. Found: C, 58.28; H, 4.82. Single crystals suitable for X-ray diffraction were grown from C_6H_6/Et_2O .

trans-Pt(Ph)(COCOME)(PPh₃)₂ (15a). Refer to **15d** for experimental details. The yield of **15a** was 42%. UV-vis (CDCl₃): λ_{max} 536 nm, ε = 108 ± 1 dm³ mol⁻¹. IR (KBr pellet): ν_{CO} 1701, 1658, 1594 cm⁻¹. ³¹P NMR (CDCl₃): δ 16.8 (*J*_{P-Pt} = 3223 Hz). ¹H NMR (CDCl₃): δ 6.50 (2H, m, Pt-C₆H₅), 6.37 (1H, m, Pt-C₆H₅), 6.30 (2H, m, Pt-C₆H₅), 0.91 (3H, s, CH₃). Anal. Calcd for PtC₄₅H₃₈O₂P₂: C, 62.28; H, 4.41. Found: C, 62.56; H, 4.34.

trans-Pt(Ph)(COCOEt)(PPh₃)₂ (15b). Refer to **15d** for experimental details. The yield of **15b** was 72%. UV-vis (CDCl₃): λ_{max} 538 nm, ε = 87 ± 1 dm³ mol⁻¹. IR (KBr pellet): ν_{CO} 1699, 1603 cm⁻¹. ³¹P NMR (CDCl₃): δ 16.7 (*J*_{P-Pt} = 3233 Hz). ¹H NMR (CDCl₃): δ 6.49 (2H, m, Pt-C₆H₅), 6.35 (1H, m, Pt-C₆H₅), 6.29 (2H, m, Pt-C₆H₅), 1.20 (2H, q, *J*_{H-H} = 7.2 Hz, CH₂), 0.35 (3H, t, *J*_{H-H} = 7.2 Hz, CH₃). Anal. Calcd for PtC₄₆H₄₀O₂P₂: C, 62.65; H, 4.57. Found: C, 62.37; H, 4.58.

trans-Pt(Ph)(COCOPh)(PPh₃)₂ (15c). Refer to **15d** for experimental details. The yield of **15c** was 40%. UV-vis (CDCl₃): λ_{max} 546 nm, ε = 123 ± 1 dm³ mol⁻¹. IR (KBr pellet): ν_{CO} 1664, 1605 cm⁻¹. ³¹P NMR (CDCl₃): δ 17.0 (*J*_{P-Pt} = 3229 Hz). ¹H NMR (CDCl₃): δ 6.47 (2H, m, Pt-C₆H₅), 6.30 (1H, m, Pt-*p*-C₆H₅), 6.20 (2H, m, Pt-C₆H₅).

trans-Pt(Ph)(COCO₂Me)(PPh₃)₂ (15d). In a round-bottom flask containing 200 mg (0.21 mmol) of *trans*-Pt(COCOME)(OTf)(PPh₃)₂ and 50 mg (0.23 mmol) of Ph₂Zn was introduced ca. 15 mL of cold dry CH₂Cl₂ under nitrogen. The mixture was allowed to react for 45 min at -5 °C. Zinc salts were first removed by adding 5 mL of ice-cooled *n*-hexane to the solution. The filtrate was concentrated to ca. 5 mL. Addition of more *n*-hexane caused the precipitation of the product. Repeated recrystallization in cold CH₂Cl₂/hexane afforded yellow crystalline **15d** in a 25% yield (46 mg). UV-vis (CDCl₃): λ_{max} 446 nm, ε = 88 ± 1 dm³ mol⁻¹. IR (KBr pellet): ν_{CO} 1720, 1612 cm⁻¹. ³¹P NMR (CDCl₃): δ 16.5 (*J*_{P-Pt} = 3197 Hz). ¹H NMR (CDCl₃): δ 6.49 (2H, m, Pt-C₆H₅), 6.36 (1H, m, Pt-C₆H₅), 6.28 (2H, m, Pt-C₆H₅), 3.02 (3H, s, OCH₃). Single crystals suitable for X-ray diffraction were grown from C_6H_6/Et_2O .

trans-Pt(CCPh)(COCOPh)(PPh₃)₂ (16c). To a benzene solution containing 20 mg of **7c** was added 2.25 μL of PhC≡CH

followed by 2.25 μL of Et₃N. Violet microcrystalline product in >90% yield was obtained after 2 days. IR (KBr pellet): ν_{C≡C} 2111 cm⁻¹. ³¹P NMR (C₆D₆): δ 16.93 (*J*_{P-Pt} = 3021 Hz). ¹H NMR (C₆D₆): δ 6.97 (3H, m, COC₆H₅), 6.27 (m, CCC₆H₅). Anal. Calcd for PtC₅₁H₄₀O₂P₂: C, 66.16; H, 4.35. Found: C, 66.60; H, 4.44. Single crystals suitable for X-ray diffraction were grown from C_6H_6/Et_2O .

cis-Pt(COCOME)(COEt)(PPh₃)₂ (17a). Refer to **17d** for experimental details. The yield of **17a** was 70–80%. UV-vis (CDCl₃): λ_{max} 504 nm, ε = 89 ± 1 dm³ mol⁻¹. IR (KBr pellet): ν_{CO} 1701, 1634, 1607 cm⁻¹. ³¹P NMR (CDCl₃): δ 14.3 (*J*_{P-P} = 20 Hz, *J*_{P-Pt} = 1571 Hz), 14.1 (*J*_{P-P} = 20 Hz, *J*_{P-Pt} = 1877 Hz). ¹H NMR (CDCl₃): δ 2.01 (2H, q, *J*_{H-H} = 7.3 Hz, CH₂ (Et)), 1.42 (3H, s, CH₃), 0.23 (3H, t, *J*_{H-H} = 7.3 Hz, CH₃ (Et)). Anal. Calcd for PtC₄₂H₃₈O₃P₂: C, 59.50; H, 4.52. Found: C, 59.04; H, 4.56. Single crystals suitable for X-ray diffraction were grown from C_6H_6/Et_2O .

cis-Pt(COCOEt)(COEt)(PPh₃)₂ (17b). Refer to **17d** for experimental details. The yield of **17b** was 70–80%. UV-vis (CDCl₃): λ_{max} 486 nm, ε = 86 ± 1 dm³ mol⁻¹. IR (KBr pellet): ν_{CO} 1703, 1642, 1615 cm⁻¹. ³¹P NMR (CDCl₃): δ 14.0 (*J*_{P-P} = 22 Hz, *J*_{P-Pt} = 1577 Hz), 13.7 (*J*_{P-P} = 22 Hz, *J*_{P-Pt} = 1861 Hz). ¹H NMR (CDCl₃): δ 2.00 (2H, q, *J*_{H-H} = 7.3 Hz, CH₂ (COEt)), 1.74 (2H, q, *J*_{H-H} = 7.2 Hz, CH₂ (COCOEt)), 0.68 (3H, t, *J*_{H-H} = 7.2 Hz, CH₃ (COCOEt)), 0.22 (3H, t, *J*_{H-H} = 7.3 Hz, CH₃ (COEt)). Anal. Calcd for PtC₄₃H₄₀O₃P₂: C, 59.92; H, 4.67. Found: C, 59.76; H, 4.60.

cis-Pt(COCOEt)(¹³COEt)(PPh₃)₂ (17c). ³¹P NMR: δ 14.0 (*J*_{P-C} = 117 Hz), 13.7 (*J*_{P-C} ≈ 16 Hz). ¹H NMR: δ 2.00 (2H, qd, *J*_{H-C} = 3.7 Hz, CH₂ (COEt)), 1.74 (2H, q, CH₂ (COCOEt)), 0.68 (3H, t, CH₃ (COCOEt)), 0.22 (3H, td, *J*_{H-C} = 4.8 Hz, CH₃ (COEt)).

cis-Pt(COCOPh)(COEt)(PPh₃)₂ (17c). Refer to **17d** for experimental details. The yield of **17c** was 75%. UV-vis (CDCl₃): λ_{max} 484 nm, ε = 168 ± 1 dm³ mol⁻¹. IR (KBr pellet): ν_{CO} 1663, 1635, 1556 cm⁻¹. ³¹P NMR (CDCl₃): δ 14.8 (*J*_{P-P} = 20 Hz, *J*_{P-Pt} = 1860 Hz), 14.1 (*J*_{P-P} = 20 Hz, *J*_{P-Pt} = 1571 Hz). ¹H NMR (CDCl₃): δ 2.08 (2H, q, *J*_{H-H} = 7.3 Hz, CH₂ (COEt)), 0.20 (3H, t, *J*_{H-H} = 7.3 Hz, CH₃ (COEt)). Anal. Calcd for PtC₄₇H₄₀O₃P₂: C, 62.04; H, 4.42. Found: C, 62.27; H, 4.30.

cis-Pt(COCOPh)(¹³COEt)(PPh₃)₂ (17c). ³¹P NMR (*d*₆-benzene): δ 14.5 (*J*_{P-C} = 93.4 Hz), 13.8 (*J*_{P-C} ≈ 8.5 Hz). ¹H NMR (*d*₆-benzene): δ 2.51 (2H, qd, *J*_{H-C} = 1.6 Hz, CH₂), 0.61 (3H, dt, *J*_{H-C} = 4.6 Hz, CH₃). An X-ray single-crystal structure with disordered -COCOPh ligand was obtained. All crystallographic data are omitted.

cis-Pt(COCO₂Me)(COEt)(PPh₃)₂ (17d). A 30 mL amount of a CH₂Cl₂ solution containing 100 mg (0.12 mmol) of **17d** was saturated with CO at 25 °C. The mixture was allowed to react for 40 min. It was then dried on a rotavap. Recrystallization from benzene/hexane gave 75 mg (73% yield) of **17d**. IR (KBr pellet): ν_{CO} 1714, 1644, 1616 cm⁻¹. ³¹P NMR (CDCl₃): δ 14.3 (*J*_{P-P} = 21 Hz, *J*_{P-Pt} = 1533 Hz), 14.0 (*J*_{P-P} = 21 Hz, *J*_{P-Pt} = 1949 Hz). ¹H NMR (CDCl₃): δ 3.38 (3H, s, OCH₃), 2.07 (2H, q, *J*_{H-H} = 7.3 Hz, CH₂ (COEt)), 0.24 (3H, t, *J*_{H-H} = 7.3 Hz, CH₃ (COEt)). Anal. Calcd for PtC₄₂H₃₈O₄P₂: C, 58.39; H, 4.43. Found: C, 57.63; H, 4.13. An X-ray single-crystal structure with unsatisfactory values of *R* and *R*_w was obtained. The poor data were due to crystal decay during the course of data collection.

cis-Pt(COCOME)(COPh)(PPh₃)₂ (18a). Refer to **18d** for experimental details. The yield of **18a** was 35–45%. UV-vis (CDCl₃): λ_{max} 414 nm, ε = 285 ± 3 dm³ mol⁻¹. IR (KBr pellet): ν_{CO} 1697, 1616, 1601 cm⁻¹. ³¹P NMR (CDCl₃): δ 14.7 (*J*_{P-P} = 21 Hz, *J*_{P-Pt} = 1702 Hz), 14.0 (*J*_{P-P} = 21 Hz, *J*_{P-Pt} = 1804 Hz). ¹H NMR (CDCl₃): δ 1.36 (3H, s, CH₃). Anal. Calcd for PtC₄₆H₃₈O₃P₂: C, 61.67; H, 4.28. Found: C, 62.24; H, 4.25. Single crystals suitable for X-ray diffraction were grown from C_6H_6/Et_2O .

cis-Pt(COCOEt)(COPh)(PPh₃)₂ (18b). Refer to **18d** for experimental details. The yield of **18b** was 40%. UV-vis (CD-

Table 3. X-ray Crystal Parameters and Data Collection

compd	3c	4b	6f	14b	15d
formula	C ₄₅ H ₄₀ O ₂ Pt	C ₄₅ H ₄₀ O ₂ Pt •CH ₂ Cl ₂	C ₄₆ H ₄₀ O ₂ Pt •0.5 C ₆ H ₆	C ₄₂ H ₄₀ O ₂ Pt •C ₆ H ₁₄	C ₄₅ H ₃₈ O ₃ Pt
fw	853.86	938.79	920.93	920.00	883.84
cryst dimns, mm	0.35 × 0.4 × 0.5	0.5 × 0.5 × 0.5	0.05 × 0.15 × 0.45	0.05 × 0.3 × 0.45	0.08 × 0.4 × 0.4
space group	P2 ₁ /c	P2 ₁ /c	P2 ₁ /c	P1̄	C2/c
a, Å	11.143(2)	12.953(7)	17.770(8)	9.779(4)	37.031(7)
b, Å	19.087(4)	16.227(5)	10.537(1)	10.936(2)	10.322(2)
c, Å	17.840(3)	19.022(8)	23.739(9)	20.151(3)	22.033(3)
α, deg	90	90	90	84.31(1)	90
β, deg	104.22(1)	90.63(4)	111.52(4)	77.28(3)	113.49(2)
γ, deg	90	90	90	87.21(3)	90
V, Å ³	3678	3998	4135	2091	7723
Z	4	4	4	2	8
ρ(calcd), g cm ⁻³	1.542	1.560	1.507	1.439	1.520
F(000)	1704	1872	1888	932	3519
radiation (λ, Å)	Mo Kα (0.7107)	Mo Kα (0.7107)	Mo Kα (0.7107)	Mo Kα (0.7107)	Mo Kα (0.7107)
T, K	300	300	300	300	300
μ, mm ⁻¹	3.97	3.79	3.79	3.50	3.79
transmissn	0.58–1.0	0.67–1.0	0.68–1.0	0.64–1.0	0.52–1.0
2θ(max), deg	45	45	45	45	45
no. of rflns measd	4792	5212	5388	5490	5030
no. of rflns obsd	3864 (>2.0σ)	3966 (>2.0σ)	2421 (>2.0σ)	4429 (>2.0σ)	3556 (>2.0σ)
no. of variables	443	469	472	425	461
R(F)	0.035	0.036	0.058	0.039	0.032
R _w (F)	0.032	0.037	0.050	0.049	0.031
S	1.60	2.08	1.27	2.92	1.21
(Δ/σ) _{max}	0.033	0.051	0.051	0.034	0.017

compd	16c	17a	18a	19b
formula	C ₅₂ H ₄₀ O ₂ Pt	C ₄₂ H ₃₈ O ₃ Pt	C ₄₆ H ₃₈ O ₃ Pt•C ₄ H ₈ O	C ₄₂ H ₄₀ O ₃ Pt•C ₆ H ₆
fw	953.91	919.90	895.83	927.92
cryst dimns, mm	0.2 × 0.2 × 0.2	0.08 × 0.3 × 0.4	0.2 × 0.25 × 0.45	0.25 × 0.35 × 0.5
space group	P2 ₁ /c	P2 ₁ /n	P1̄	P2 ₁ /c
a, Å	13.217(2)	17.116(2)	11.043(3)	12.311(3)
b, Å	9.459(2)	10.625(3)	11.342(5)	14.344(4)
c, Å	33.802(4)	23.878(6)	18.125(7)	24.547(6)
α, deg	90	90	98.92(3)	90
β, deg	94.58(1)	110.887(2)	96.23(3)	102.48(2)
γ, deg	90	90	117.26(3)	90
V, Å ³	4213	4057	1951	4232
Z	4	4	2	4
ρ(calcd), g cm ⁻³	1.504	1.506	1.525	1.456
F(000)	1904	1848	892	1864
radiation (λ, Å)	Cu Kα (1.5418)	Mo Kα (0.7107)	Mo Kα (0.7107)	Mo Kα (0.7107)
T, K	300	300	300	300
μ, mm ⁻¹	7.33	3.61	3.75	3.46
transmissn	0.87–1.0	0.69–1.0	0.72–1.0	0.84–1.0
2θ(max), deg	120	45	45	45
no. of rflns measd	6256	5304	5130	5518
no. of rflns obsd	5571 (>2.5σ)	3586 (>2.0σ)	4279 (>2.0σ)	4138 (>2.0σ)
no. of variables	514	479	439	488
R(F)	0.048	0.039	0.042	0.028
R _w (F)	0.060	0.035	0.045	0.022
S	2.23	1.21	2.13	1.84
(Δ/σ) _{max}	0.000	0.059	0.042	0.048

Cl₃): λ_{max} 428 nm, ε = 234 ± 3 dm³ mol⁻¹. IR (KBr pellet): ν_{CO} 1701, 1624, 1602 cm⁻¹. ³¹P NMR (CDCl₃): δ 14.9 (J_{P-P} = 22 Hz, J_{P-Pt} = 1706 Hz), 13.6 (J_{P-P} = 22 Hz, J_{P-Pt} = 1786 Hz). ¹H NMR (CDCl₃): δ 1.70 (2H, q, J_{H-H} = 7.2 Hz, CH₂), 0.59 (3H, t, J_{H-H} = 7.2 Hz, CH₃). Anal. Calcd for PtC₄₇H₄₀O₃P₂: C, 62.04; H, 4.42. Found: C, 62.27; H, 4.30.

cis-Pt(COCOPh)(COPh)(PPh₃)₂ (18c). Refer to 18d for experimental details. The reaction was performed at 0 °C, and mixed products were recovered. UV-vis (C₆H₆): λ_{max} 450 nm, ε = 120 ± 1 dm³ mol⁻¹. IR (KBr pellet): ν_{CO} 1668, 1601, 1555 cm⁻¹. ³¹P NMR (C₆D₆): δ 16.5 (J_{P-P} = 20 Hz, J_{P-Pt} = 1696 Hz), 13.1 (J_{P-P} = 20 Hz, J_{P-Pt} = 1733 Hz). ¹H NMR (C₆D₆): δ 6.7–7.9 (m, phenyl H).

cis-Pt(COCO₂Me)(COPh)(PPh₃)₂ (18d). A 40 mL amount of a CH₂Cl₂ solution containing 60 mg (0.12 mmol) of 18d was saturated with CO at 30 °C. The solution was vigorously stirred for 40 min. It was dried on a rotavap. Recrystallization from benzene/hexane gave 35 mg (57% yield) of 18d. IR (KBr pellet): ν_{CO} 1715, 1653, 1608 cm⁻¹. ³¹P NMR (CDCl₃): δ 14.2

(J_{P-P} = 21 Hz, J_{P-Pt} = 1646 Hz), 13.7 (J_{P-P} = 21 Hz, J_{P-Pt} = 1882 Hz). ¹H NMR (CDCl₃): δ 3.33 (3H, s, OCH₃).

trans-Pt(COMe)(OCOME)(PPh₃)₂ (19a). Refer to 19b for experimental details. The yield of orange 19a was 57%. UV-vis (C₆H₆): λ_{max} 480 nm, ε = 68 ± 1 dm³ mol⁻¹. IR (KBr pellet): ν_{CO} 1652, 1611 cm⁻¹. ³¹P NMR (C₆D₆): δ 19.06 (J_{P-Pt} = 3629 Hz). ¹H NMR (C₆D₆): δ 1.38 (3H, s, CH₃ (OCOME)), 1.21 (3H, s, CH₃ (COMe)).

trans-Pt(COEt)(COEt)(PPh₃)₂ (19b). In a 25 mL round-bottom flask, 80 mg of 14b (0.095 mmol) was allowed to decompose in 10 mL of benzene at room temperature. After 2 days, the reaction solution was concentrated to about 2 mL. Introducing ice-cold *n*-hexane into it resulted in a yellow precipitate. Repeated crystallization from benzene/*n*-hexane gave 19b in 50% yield. IR (KBr pellet): ν_{CO} 1600, 1642 cm⁻¹. ³¹P NMR (C₆D₆): δ 19.5 (J_{P-Pt} = 3661 Hz). ¹H NMR (C₆D₆): δ 1.80 (2H, q, J_{H-H} = 7.1 Hz, J_{H-P} = 8.3 Hz, CH₂ (COEt)), 1.51 (2H, q, J_{H-H} = 7.6 Hz, J_{H-Pt} = 13.4 Hz, CH₂ (COEt)), 0.66 (3H, t, J_{H-H} = 7.6 Hz, J_{H-P} = 3.7 Hz, J_{H-Pt} = 13.1 Hz, CH₃

Table 4. Selected Bond Distances (Å) and Angles (deg)

<i>trans</i> -Pt(COPh)(Et)(PPh ₃) ₂ (3c)							
Pt–P1	2.268(2)	C1–C2	1.51(1)	Pt–C1	2.155(6)	C3–O	1.251(8)
Pt–P2	2.280(2)	C3–C4	1.52(1)	Pt–C3	2.063(7)		
P1–Pt–P2	168.14(6)	C1–Pt–C3	168.1(3)	P1–Pt–C3	93.4(2)	Pt–C3–C4	126.4(5)
P1–Pt–C1	86.2(2)	Pt–C1–C2	118.3(5)	P2–Pt–C1	89.1(2)	Pt–C3–O	117.8(5)
				P2–Pt–C3	93.4(2)	C4–C3–O	115.8(6)
<i>trans</i> -Pt(COEt)(Ph)(PPh ₃) ₂ (4b)							
Pt–P1	2.301(2)	O–C1	1.24(1)	Pt–C1	2.055(9)	C2–C3	1.49(1)
Pt–P2	2.291(2)	C1–C2	1.51(1)	Pt–C4	2.115(8)		
P1–Pt–P2	177.21(8)	Pt–C1–O	122.9(6)	P2–Pt–C1	92.1(2)	C1–C2–C3	117.2(8)
P1–Pt–C1	90.7(2)	Pt–C1–C2	119.1(6)	P2–Pt–C4	87.9(2)	Pt–C4–C5	121.7(7)
P1–Pt–C4	89.4(2)	O–C1–C2	118.0(8)	C1–Pt–C4	177.4(4)	Pt–C4–C9	122.5(6)
<i>cis</i> -Pt(COEt)(COPh)(PPh ₃) ₂ (6f)							
Pt–P1	2.329(6)	C1–O1	1.21(2)	Pt–C4	1.98(3)	C4–C5	1.50(4)
Pt–P2	2.329(6)	C2–C3	1.46(3)	C1–C2	1.48(3)	C5–C6	1.35(4)
Pt–C1	2.10(2)	C4–O2	1.24(3)				
P1–Pt–P2	100.5(2)	Pt–C1–O1	121(2)	P2–Pt–C4	88.5(7)	Pt–C4–O2	122(2)
P1–Pt–C1	89.2(5)	C2–C1–O1	124(2)	C1–Pt–C4	81.6(9)	C5–C4–O2	111(3)
P1–Pt–C4	168.9(7)	C1–C2–C3	116(2)	Pt–C1–C2	115(1)	C4–C5–C6	113(2)
P2–Pt–C1	170.0(5)	Pt–C4–C5	126(2)				
<i>trans</i> -Pt(COCOEt)(Et)(PPh ₃) ₂ (14b)							
Pt–P1	2.287(3)	C1–O1	1.18(2)	Pt–C5	2.11(1)	C3–C4	1.42(3)
Pt–P2	2.272(3)	C2–C3	1.46(2)	C1–C2	1.53(2)	C5–C6	1.53(2)
Pt–C1	2.05(1)	C2–O2	1.22(2)				
P1–Pt–P2	177.0(1)	Pt–C1–O1	132(1)	P2–Pt–C5	86.1(3)	C3–C2–O2	119(1)
P1–Pt–C1	88.3(3)	C2–C1–O1	111(1)	C1–Pt–C5	175.6(5)	C2–C3–C4	122(2)
P1–Pt–C5	92.9(3)	C1–C2–C3	120(1)	Pt–C1–C2	117.3(8)	Pt–C5–C6	113.2(8)
P2–Pt–C1	92.9(3)	C1–C2–O2	120(1)				
<i>trans</i> -Pt(COCOME)(Ph)(PPh ₃) ₂ (15d)							
Pt–P1	2.288(2)	C1–O1	1.181(9)	Pt–C4	2.087(8)	C3–O3	1.46(1)
Pt–P2	2.288(2)	C2–O2	1.196(9)	C1–C2	1.57(1)		
Pt–C1	2.069(7)	C2–O3	1.310(9)				
P1–Pt–P2	173.12(8)	Pt–C1–O1	129.9(6)	P2–Pt–C4	91.1(2)	O2–C2–O3	123.6(7)
P1–Pt–C1	93.1(2)	C2–C1–O1	117.3(7)	C1–Pt–C4	175.9(3)	Pt–C4–C5	119.7(6)
P1–Pt–C4	86.0(2)	C1–C2–O2	123.2(7)	Pt–C1–C2	112.8(5)	Pt–C4–C9	125.5(6)
P2–Pt–C1	90.2(2)	C1–C2–O3	113.2(6)				
<i>trans</i> -Pt(COCOPh)(C≡CPh)(PPh ₃) ₂ (16c)							
Pt–P1	2.291(2)	C1–C2	1.53(1)	Pt–C9	2.058(6)	C9–C10	1.13(1)
Pt–P2	2.298(2)	O2–C2	1.25(1)	O1–C1	1.25(1)	C10–C11	1.46(1)
Pt–C1	2.032(7)	C2–C3	1.52(1)				
P1–Pt–P2	177.00(7)	Pt–C1–C2	119.8(5)	P2–Pt–C9	86.0(2)	C1–C2–C3	120.9(7)
P1–Pt–C1	91.0(2)	O1–C1–C2	114.2(6)	C1–Pt–C9	176.8(3)	Pt–C9–C10	171.1(7)
P1–Pt–C9	92.2(2)	O2–C2–C1	118.0(7)	Pt–C1–O1	125.7(6)	C9–C10–C11	175.1(9)
P2–Pt–C1	90.9(2)	O2–C2–C3	121.0(7)				
<i>cis</i> -Pt(COCOME)(COEt)(PPh ₃) ₂ (17a)							
Pt–P1	2.331(2)	C1–O1	1.21(1)	Pt–C4	2.070(8)	C4–C5	1.51(1)
Pt–P2	2.341(3)	C2–C3	1.47(2)	C1–C2	1.50(2)	C5–C6	1.49(1)
Pt–C1	2.03(1)	C2–O2	1.14(2)				
P1–Pt–P2	99.57(9)	Pt–C1–O1	129.2(8)	P2–Pt–C4	89.9(3)	C3–C2–O2	123(1)
P1–Pt–C1	90.8(3)	C2–C1–O1	113.8(9)	C1–Pt–C4	79.8(4)	Pt–C4–C5	116.0(6)
P1–Pt–C4	170.4(3)	C1–C2–C3	115(1)	Pt–C1–C2	116.9(7)		
P2–Pt–C1	169.6(3)	C1–C2–O2	122(1)				
<i>cis</i> -Pt(COCOME)(COPh)(PPh ₃) ₂ (18a)							
Pt–P1	2.335(3)	C2–C3	1.47(2)	Pt–C4	2.052(9)	C5–C6	1.40(1)
Pt–P2	2.363(3)	C2–O2	1.15(2)	C1–C2	1.54(2)	C4–O3	1.22(1)
Pt–C1	1.999(9)	C4–C5	1.49(1)	C1–O1	1.22(1)		
P1–Pt–P2	101.3(1)	C2–C1–O1	115.8(9)	P2–Pt–C4	89.6(3)	Pt–C4–C5	119.9(6)
P1–Pt–C1	91.1(3)	C1–C2–C3	117(1)	C1–Pt–C4	78.1(4)	Pt–C4–O3	122.2(7)
P1–Pt–C4	169.1(3)	C1–C2–O2	122(1)	Pt–C1–C2	114.2(7)	C5–C4–O3	117.9(8)
P2–Pt–C1	165.2(3)	C3–C2–O2	121(1)	Pt–C1–O1	130.0(8)		
<i>trans</i> -Pt(OCOEt)(COEt)(PPh ₃) ₂ (19b)							
Pt–P1	2.302(2)	O3–C4	1.201(7)	Pt–C4	1.989(6)	C4–C5	1.524(9)
P5–P2	2.301(2)	C1–C2	1.493(8)	O1–C1	1.279(7)	C5–C6	1.509(9)
P5–O1	2.142(4)	C2–C3	1.44(1)	O2–C1	1.230(8)		
P1–Pt–P2	169.97(6)	O1–C1–C2	114.5(6)	P2–Pt–C4	93.2(2)	Pt–C4–C5	113.8(4)
P1–Pt–O1	93.1(1)	O2–C1–C2	121.0(6)	O1–Pt–C4	175.9(2)	O3–C4–C5	118.9(5)
P1–Pt–C4	88.5(2)	C1–C2–C3	117.1(7)	Pt–O1–C1	114.2(4)	C4–C5–C6	115.3(5)
P2–Pt–O1	86.0(1)	Pt–C4–O3	127.3(5)	O1–C1–O2	124.4(5)		

(COEt)), 0.24 (3H, t, $J_{\text{H-H}} = 7.1$ Hz, $J_{\text{H-Pt}} = 11.8$ Hz, CH_3 (OCOEt)). Anal. Calcd for $\text{PtC}_{42}\text{H}_{40}\text{O}_3\text{P}_2$: C, 59.36; H, 4.74. Found: C, 59.90; H, 4.74. Single crystals suitable for X-ray diffraction were grown from benzene/toluene/*n*-hexane.

trans-Pt(COPh)(OCOPh)(PPh₃)₂ (19c). Refer to **19b** for experimental details. The isolated yield of **19c** was 42%. IR (KBr pellet): ν_{CO} 1648, 1605 cm^{-1} . ^{31}P NMR (C_6D_6): δ 19.90 ($J_{\text{P-Pt}} = 3648$ Hz). ^1H NMR (C_6D_6): δ 6.8–8.0 (m, phenyl H).

trans-Pt(COMe)(OCOEt)(PPh₃)₂ (19d) and trans-Pt(COEt)(COMe)(PPh₃)₂ (19d'). Refer to **19b** for experimental details. Mixtures of **19d** and **19d'** were characterized by NMR spectroscopy. **19d**: ^{31}P NMR (C_6D_6) δ 19.55 ($J_{\text{P-Pt}} = 3655$ Hz); ^1H NMR (C_6D_6) δ 1.80 (2H, q, $J_{\text{H-H}} = 7.2$ Hz, CH_2 (Et)), 1.25 (3H, s, CH_3 (Me)), 0.24 (3H, t, $J_{\text{H-H}} = 7.2$ Hz, CH_3 (Et)). **19d'**: ^{31}P NMR (C_6D_6) δ 19.48 ($J_{\text{P-Pt}} = 3655$ Hz); ^1H NMR (C_6D_6) δ 1.51 (2H, q, $J_{\text{H-H}} = 7.4$ Hz, CH_2 (Et)), 1.40 (3H, s, CH_3 (Me)), 0.66 (3H, t, $J_{\text{H-H}} = 7.4$ Hz, CH_3 (Et)).

trans-Pt(COMe)(OCOPh)(PPh₃)₂ (19e) and trans-Pt(COPh)(OCOMe)(PPh₃)₂ (19e'). Using **18a** as the starting material, the mixture of **19e** and **19e'** was characterized by NMR spectroscopy. **19e**: ^{31}P NMR (C_6D_6) δ 19.48 ($J_{\text{P-Pt}} = 3596$ Hz); ^1H NMR (C_6D_6) δ 1.22 (3H, s, CH_3 (COMe)). **19e'**: ^{31}P NMR (C_6D_6) δ 19.04 ($J_{\text{P-Pt}} = 3552$ Hz); ^1H NMR (C_6D_6) δ 1.40 (3H, s, CH_3 (OCOMe)).

trans-Pt(COEt)(OCOPh)(PPh₃)₂ (19f) and trans-Pt(COPh)(OCOEt)(PPh₃)₂ (19f'). The mixture of **19f** and **19f'** was characterized by NMR spectroscopy. **19f**: ^{31}P NMR (C_6D_6) δ 19.89 ($J_{\text{P-Pt}} = 3653$ Hz); ^1H NMR (C_6D_6) δ 1.56 (2H, q, $J_{\text{H-H}} = 7.6$ Hz, CH_2 (Et)), 0.66 (3H, t, $J_{\text{H-H}} = 7.6$ Hz, CH_3 (Et)).

trans-Pt(OCOPh)(¹³COEt)(PPh₃)₂: ^1H NMR (*d*₆-benzene) δ 1.56 (2H, qd, $J_{\text{H-C}} = 2.1$ Hz, CH_2), 0.66 (3H, dt, $J_{\text{H-C}} = 4.5$ Hz, CH_3). **19f'**: ^{31}P NMR (C_6D_6) δ 19.55 ($J_{\text{P-Pt}} = 3654$ Hz); ^1H NMR (C_6D_6) δ 1.81 (2H, q, $J_{\text{H-H}} = 7.1$ Hz, CH_2 (Et)), 0.23 (3H, t, $J_{\text{H-H}} = 7.1$ Hz, CH_3 (Et)).

trans-Pt(COPh)(O¹³COEt)(PPh₃)₂: ^1H NMR (C_6D_6) δ 1.81 (2H, qd, $J_{\text{H-C}} = 1.6$ Hz, CH_2), 0.23 (3H, dt, $J_{\text{H-C}} = 3.8$ Hz, CH_3).

X-ray Crystallographic Analysis. Diffraction data were measured on a Nonius CAD-4 diffractometer. Cell parameters were determined by a least-squares fit of 25 reflections. Intensity data were corrected for absorption on the basis of an experimental ψ rotation curve. The refinement procedure was by a full-matrix least-squares method including all the non-hydrogenic atoms anisotropically. Hydrogen atoms were fixed at ideal geometry and a C–H distance of 1.0 Å; their isotropic thermal parameters were fixed at the values of the attached carbon atoms at the convergence of the isotropic refinement. Atomic scattering factors were taken from ref 29. Computing programs are from the NRC VAX package.³⁰ Crystallographic data and the selected bond parameters of **3c**, **4b**, **6f**, **14b**, **15d**, **16c**, **17a**, **18a**, and **19b** are listed in Tables 3 and 4. Other detailed data for these complexes and the data for **4c**, **5c**, **13a**, **14d**, and **17d** are supplied in the supplementary material.

Acknowledgment. We gratefully thank the National Science Council, Taipei, Taiwan, ROC, for the financial support. The help in (500 MHz) NMR measurements by Miss S.-C. Lin and Dr. D.-K. Chang of the Institute of Chemistry, Academia Sinica, Nankang, ROC, is acknowledged.

Supplementary Material Available: Text giving X-ray crystal parameters and details of data collection, fully labeled ORTEP drawings, and tables of atomic coordinates, complete bond lengths and bond angles, and thermal parameters of **3c**, **4b,c**, **5c**, **6f**, **13a**, **14b,d**, **15d**, **16c**, **17a,d**, **18a**, and **19f** (112 pages). Ordering information is given on any current masthead page.

OM940653M

(29) *International Tables for X-Ray Crystallography*; Kynoch Press: Birmingham, U.K., 1974; Vol. IV.

(30) NRC VAX: Gabe, E. J.; LePage, Y.; Charland, J.-P.; Lee, F. L.; White, P. S. *J. Appl. Crystallogr.* **1989**, *22*, 384.